Advanced Materials

Lipid and nucleic acid chemistries: combining the best of both worlds to construct advanced materials

--Manuscript Draft--

Manuscript Number:	
Full Title:	Lipid and nucleic acid chemistries: combining the best of both worlds to construct advanced materials
Article Type:	Invited Progress Report
Section/Category:	
Keywords:	Nucleosides, Lipids, Amphiphiles, supramolecular assemblies, Hydrogels
Corresponding Author:	Philippe Antoine Barthelemy, Prof. Dr. Universite de Bordeaux Bordeaux Cedex,, FRANCE
Additional Information:	
Question	**Response**
Please submit a plain text version of your cover letter here. **If you are submitting a revision of your manuscript, please do not overwrite your original cover letter. There is an opportunity for you to provide your responses to the reviewers later; please do not add them here**.	September 5, 2017 Dear Editor: Following your letter of invitation, please find attached a pdf file of our manuscript entitled "Lipid and nucleic acid chemistries: combining the best of both worlds to construct advanced materials " which we submit for your consideration as a progress report. This manuscript presents recent advances in the chemistry, biophysics and biology of hybrid nucleolipid based amphiphiles. The supramolecular materials generated by these molecules open new challenges for applications in the field of science and technology for health. This progress report should be of interest to many interdisciplinary scientists working in a wide range of scientific areas involving soft materials and we believe that Advanced Materials is the appropriate journal for publication of this report. Thank you for your consideration. Sincerely yours, Philippe Barthélémy
Do you or any of your co-authors have a conflict of interest to declare?	No. The authors declare no conflict of interest.
Corresponding Author Secondary Information:	
Corresponding Author's Institution:	Universite de Bordeaux
Corresponding Author's Secondary Institution:	
First Author:	Philippe Antoine Barthelemy, Prof. Dr.
First Author Secondary Information:	
Order of Authors:	Philippe Antoine Barthelemy, Prof. Dr.
	Julie Baillet
	valerie Desvergnes, PhD
	Aladin Hamoud

	Laurent Latxague, PhD
Order of Authors Secondary Information:	

WILEY-VCH

DOI: 10.1002/((please add manuscript number))
Article type: Progress Reports

Lipid and nucleic acid chemistries: combining the best of both worlds to construct advanced materials

*Julie Baillet‡, Valérie Desvergnes‡, Aladin Hamoud, Laurent Latxague, and Philippe Barthélémy**

Julie Baillet, Dr. Valérie Desvergnes, Aladin Hamoud, Dr. Laurent Latxague, Pr. Philippe Barthélémy
ARNA Laboratory, Inserm, U1212, CNRS 5320,
Université de Bordeaux, F-33000, Bordeaux, France.
E-mail: philippe.barthelemy@inserm.fr

‡ Julie Baillet and Valérie Desvergnes contributed equally to this work.

Keywords: Nucleosides, Lipids, Amphiphiles, supramolecular assemblies, Hydrogels

Abstract. Hybrid synthetic amphiphilic biomolecules are emerging as promising supramolecular materials for biomedical and technological applications. Herein, we highlight recent progress in the field of nucleic acid-based lipids with an emphasis on their molecular design, synthesis, supramolecular properties, physico-chemical behaviors and their applications in the field of science and technology for health. In the first section we focus on the design and the study of nucleolipids, then the glycosyl-nucleolipids family is discussed. In the last section, we describe recent contributions on responsive materials involving nucleolipids and their use as smart drug delivery systems. The supramolecular materials generated by nucleic acid based lipids open new challenges for biomedical applications, including in the fields of medicinal chemistry, biosensors, biomaterials for tissue engineering, drug delivery and decontamination of nanoparticles.

1. Introduction

In the last twenty years, research on materials for biomedical applications has been mainly focused on the fabrication of maters that confer properties of interest (biocompatibility,

biodegradability, stiffness, sustainability, among others) to a device or a system. A fundamental principle has been to modulate the material properties depending upon the application requirement by assembling together most of the time different polymers. Nowadays, we are currently witnessing a paradigm shift with novel materials derived from non-polymeric small molecules that can adapt to environment and actively perform tasks depending on the conditions and/or stimuli. In the field of biomedicine, the next-generation of materials will be designed to actively perform complex functions or task in biological environments. Nature is providing many examples of such materials, which are composed of supramolecular assemblies involving biomolecules, including nucleic acids, peptide, oligosaccharides, lipids, etc. In this regard, bioinspired supramolecular materials designed using basic supramolecular principles, including hydrogen bonding, metal chelation, hydrophobic effects, π-π interactions, and/or van der Waals interactions are of major interest for application in the field of science and technology for health.

Interestingly, synthetic biomolecules can mimic many properties of their biological analogues. Hence, novel bioinspired chemical structures are currently under investigation in order to address a broad range of demands in different areas of biomedicine, including molecular and nanoscience, regenerative medicine, drug delivery or bioimaging. In this regard, materials designed *via* the synthetic combination of biological units such as lipids, nucleic acids and/or sugar represent a simple approach to create new functionalities and new biological mechanical properties. Here, recent advances in synthesis and applications of hybrid nucleolipids and glyconucleolipids will be described, with a particular attention toward molecular, supramolecular and biological properties. Some potential uses of these hybrid biomolecules within the disciplines of nanotechnologies and supramolecular biomaterials, will be highlighted.

In this contribution, we will review the recent progress in the synthesis and studies of

hybrid nucleolipids. We will mainly focus on nucleolipids (NLs, nucleoside and nucleotide-lipids) and glyconucleolipids (GNLs and bolaamphiphiles), as we believe these families present promising potentials in the field of health science and technology. We will further highlight recent contributions involving responsive NLs and impressive applications of these materials in soft material engineering and drug delivery. Finally, some anticipated challenges related to the development of the next generation of nucleic acid based lipids will be discussed.

2. Nucleolipids

Generally speaking, NLs are hybrid molecules combining a nucleobase, nucleoside, nucleotide with a lipophilic part **(Figure 1)**.[1–4] Hybrid lipid-nucleoside or nucleotide compounds can be natural occurring in eucaryotic and procaryotic cells. During the last several years, synthetic chemists have devoted efforts to combine the potential biological functions and activities of nucleosides and nucleotides with the self-assembling properties of lipids. Original NLs were designed and synthesized to investigate the impact of molecular structural modifications on the physico-chemical and subsequently aggregation properties. A wide panel of novel amphiphilic NLs has been reported which could be classified according various criteria: charge, substitution position (2' and 3', 5', onto the base), structural composition (nucleoside or nucleotide), shape (bola form for example). Synthetic methods providing both nucleoside-lipid and nucleotide-lipid conjugates and their applications reported since 2010 will be first explored herein. Approaches involving Lipid-oligonucleotides (LON) will not be discussed here. The following reported compounds have been selected on the basis of their structural originality, for their interest as new materials or for further potential applications.

2.1. Nucleoside lipids

2.1.1. Nucleoside-lipids synthesized via esters, amides, ether, amine or sulfur functions

Since 2010, only few approaches to synthetic nucleoside-lipid have been reported. Most of them involve very simple linker functions such as esters, ethers or amides links at various positions on the sugar ring (2', 3', 5') or anchored on the nucleobase.

In 2011, polyacylated Thymidine or Uridine-based NLs were synthesized and studied for potential applications as nanovectors in drug delivery.[5] In order to induce self-assembly in aqueous solutions, NLs were built from a Thymidine or Uridine central scaffold, bearing - one pyridine arm inserted at the *N*-3 position of the base, - one hydrophilic oligo(ethylene glycol) linked at the 5'-OH ribose group, expected to optimize the hydrophilic/lipophilic balance and - one or two (case of Uridine) lipophilic oleyl chains attached to the ribose secondary hydroxyl group(s) **(Figure 2)**. Classical coupling reaction conditions were used to introduce first the oleyl residue at the 2'-OH position and secondly the oligo(ethylene glycol) chain at the 5'-OH position. For that purpose, triethylene glycol (TEG) and hexaethylene glycol (HEG) were used as starting materials for acids derivatives **(Figure 2A)**. **ToThy 2**, **HoThy 3** and **DoHu 4** compounds respectively were obtained in good overall yields over a four-step sequence (41-48%) and dissolved in pure water (or a phosphate buffer) to allow the formation of large aggregates, which were analyzed by dynamic light scattering (DLS). Under pseudo-physiological conditions, multilayer vesicles presence was highlighted. The radius of these vesicles was smaller in buffer than when measured in pure water, the presence of salts enhancing the formation of packed structures of alkyl chains **(Figure 2B)**. Bioactivity and *in vitro* cytotoxicity were investigated revealing the absence of significant toxicity on both normal and tumor cells for **HoThy 3** and **DoHu 4** making them both very interesting candidate carriers to incorporate metal complexes based drugs using pyridine arm as a ligand **(Figure 2C)**.

To go further and following the same approach on a Thymidine central scaffold, the authors used the pyridine methyl arm as ruthenium ligand to provide an octaedric complex with Ru(III) cation **(Figure 3)**. By this way, AziRu bioactive complex was inserted into a nucleoside-lipid scaffold **(Figure 3A frame)**. The synthesis of an original cholesterol-based Thymidine-NL ruthenium complex named **ToThyCholRu 5** stabilized by lipid aggregates for antineoplastic therapy was reported **(Figure 3A)**.[6] Indeed, ruthenium derivatives have emerged as promising alternatives to Pt-based cisplatin chemotherapeutic drugs.[7] To increase its stability in aqueous medium, this original **ToThyCholRu** ruthenium complex **5** was incorporated into the phospholipid membrane of a liposome bilayer formed by the naturally occurring lipid 1-palmitoyl-2-oleyl-*sn*-glycero-3-phosphocholine (POPC) leading to a lesser degradation of Ru aggregates. As shown in **Figure 3B**, the cholesterol residue was inserted inside the bilayer whereas the metal Ru head was lodged between phospholipid hydrophilic heads. Effect of ToThyCholRu/POPC liposomes onto the cellular viability of two human cancer cell lines (WiDr epithelial colorectal adenocarcinoma cells and MCF-7 breast adenocarcinoma cells) was explored. With lower IC_{50} values (half maximal inhibitory concentration) ToThyCholRu/POPC exhibited a better inhibiting activity against human cancer cells than the reference Ru-complex AziRU **(Figure 3C)**. This exciting result demonstrates that the nucleoside lipid structure or scaffold can improve the anticancer activity of drugs.

A series of Ruthenium-based complex nanocarriers were subsequently designed for cancer therapy. **ToThyRu 6** and **HoThyRu 7** represented below are based on a Thymidine and **DoHuRu 8** on a Uridine structure **(Figure 4)**.[8] The poly functional nucleoside scaffold was decorated with one or two oleic acid chains (2' and 3' positions) and with an oligo(ethylene oxide) at 5' position as previously described allowing amphiphilic properties to the resulting edifice **(Figure 4A)**. Ruthenium complexes derivatives were found to exhibit

self-aggregation behavior forming liposomes among other things. Dynamic Light Scattering (DLS) studies suggested that ternary systems exhibited the presence of a single translational diffusive species **(Figure 4B)**. The average ~60nm R_H value in the same range as the one obtained for pure POPC based liposomes suggested that there was no micelles formation and that Ru complexes were inserted into the liposome bilayer without leading to its destabilization. Interestingly, their stable formulations in POPC, as innovative vectorization systems, exhibited high promising in vitro antiproliferative activities on different cancer cell lines, including MCF-7 human breast adenocarcinoma cells, WiDr human colorectal adenocarcinoma cells and Tumor C6 rat glioma cells.

In order to take full advantage of the nucleobase recognition ability, the same authors developed the synthesis of a second generation of NL-based Ru complexes where the pyridine ligand was not anchored at the *N*-3 position but at the 3'-position of the sugar moiety **(Figure 5)**.[9] The key intermediate was here the 3'-azido-3'-deoxy-1-β-D-xylofuranosyluracil **9**[10] which was substituted following the same global modular strategy as previously described to provide **HoUrRu 10** complex in a 7-step sequence and in 35% overall yield.

This compound was shown to co-aggregate with either POPC (up to 15% mol) or DOTAP (***N***-[1-(2,3-Dioleoyloxy)propyl]-*N*,*N*,*N*-trimethylammonium chloride) (up to 50% mol) to provide stable formulations in physiological media. POPC/HoUrRu and DOTAP/HoUrRu aggregates have been characterized by DLS, small angle neutron scattering (SANS) and electron paramagnetic resonance (EPR) analyses and it was highlighted that HoUrRu displayed enhanced ability to co-aggregate with various lipids. Moreover, in vitro inhibition properties of aggregates against human cancer cells MCF-7 and WiDr proved to be much more effective than the reference AziRu complex and exhibited the best activity against WiDr cells compared to previously cited Ru complexes. Such Nucleoside lipid-Ru complexes are undoubtedly very original and promising *in vivo* drug carriers.[11]

In 2010, Drummond *and coll.* reported the synthesis of three non-ionic Thymidine-based NLs: 3'-oleylthymidine **11**, 3'-phytanoylthymidine **12**, 3',5'-dioleylthymidine **13** and the study of their physical properties **(Figure 6A)**.[12] In particular, their phase behavior in aqueous media was explored using microscopy techniques and small-angle X-ray scattering (SAXS). As expected, hydroxyl group at the 5' position in 3'-oleylthymidine **11** and in 3'-phytanoylthymidine **12** seemed to be essential for the polar head hydrophobicity in water, which led to a lyotropic phase at room temperature. In contrast 3',5'-dioleylthymidine **13** was non water swelling under the same conditions. Transmission electron microscopy (TEM) of spherulites from 3'-oleylthymidine **11** showed fibrils **(Figure 6B)**. The authors concluded that, regarding to their size and surface area/volume ratio, such fibrils organizations should be useful to provide carrier vehicles for encapsulation and controlled release of agents. The ability of the three synthetic derivatives to bind single-stranded DNA oligomers in a monolayer film form was explored using a Langmuir trough **(Figure 6C)**. Thymidine NLs were evaluated for their specificity for Adenosine complementary 10-base oligomer. The behavior of both 3'-substituted compounds was found to be similar. The molecular surface at monolayer collapse in presence of DNA oligomers (polyAdenosine and polyThymidine) was shown to increase, indicating interaction between monolayers of both 3'-monosubstituted NLs and DNA oligomers at the air-water interface. This interaction emphasis is particularly promising for the use of these readily accessible simple NLs as transfection agents.

Liebscher *and coll*. reported in 2010 a straightforward synthesis of 2'-substituted Uridine using a Cu-catalyzed azide-alkyne cycloaddition (CuAAC) to introduce various groups of biological interest such as lipids, fluorophore, lysine, biotin or glycoside **(Figure 7)**.[13] Spectroscopic studies were used to investigate the anchorage of cholesterol-derivatives into POPC membranes.

The distribution of the different sugar, Uridine and triazole parts of the NL in the membrane was investigated using two-dimensional ^{1}H magic angle spinning (MAS) NOESY NMR spectroscopy. Cross-relaxation rate values could be closely linked to the contact probability between the different molecular groups and revealed that they were localized within the lipid/water interface region of the membrane. NMR spectroscopy investigations probed the anchorage of 2'-triazole substituted NLs in lipid membranes without affecting the molecular order in bilayers.

Very recently, Srivatsan *and coll.* reported the synthesis of very simple Thymidine based NLs as innovative materials with surface tunability and metal ion responsiveness **(Figure 8A)**.[14] Two types of fatty acid substituted NLs were synthesized and studied. 3',5'-*O*-disubstituted compounds were found to exhibit organogelation properties in various pure organic solvents. Conversely, in the case of 3'-monosubstituted NLs, presence of water in the organic solvent was required to induce the formation of stable gels excepted in the case of unsaturated oleyl chain which did not gel whatever the solvent conditions used **(Figure 8B, Figure 8C)**. The morphology of these various xerogels was studied using field emission scanning electron microscopy (FESEM) showing the formation of long sheets for 3'-monosubstituted NLs whereas 3',5'-*O*-disubstituted compounds formed long ribbons indicating that different gelation mechanisms were involved **(Figure 8B, Figure 8C)**. Crystal structure analysis, power X-ray diffraction (PXRD), and NMR studies indicated that for 3'-*O*-palmitoyl NLs, hydrophobic effects between lipidic tails and polar interactions between the nucleobase combined with hydrogen bonding with water were responsible for gelation properties. It was demonstrated that the nature of the solvent mixture used for gelation, influencing the possible orientation of fatty tails, was crucial in the surface property tuning which was efficiently switched from hydrophobic to hydrophilic **(Figure 8B)**.

Introduction of small amounts of Hg^{2+} cation was shown to disrupt 3',5'-*O*-distearoyl Thymidine gelation which was clearly visible by the degradation of twisted long ribbons on scanning electron microscopy (SEM) images represented below **(Figure 8C)**. NMR analyses indicated that the cation should have displaced the H bonding involved in the supramolecular assembling to form a Thymidine-Hg-Thymidine pair. This publication is a very nice example of physico-chemical properties tuning by design of NL structure.

Regarding nucleoside lipids connected *via* ether linkage, several structures have been investigated. Rosenmeyer's team, which has an extensive experience in the synthesis and biological evaluation of NLs reported lipidic prodrugs derivatives using a 5-fluorouridine **15** as starting material **(Figure 9)**. A large number of lipophilic prodrugs of 5-fluorouracil and its nucleosides derivatives have been found to exhibit antitumor activity. In this context, Rosenmeyer *and coll.* reported an access to a series of cyclic **16a-g** and acyclic *O*-2',3'-ketal derivatives **17a-c** using various cyclic and linear ketones (including heptan-4-one, ethyl levulinate, norbornan-2-one, adamantan-2-one, cycloheptanone, cyclooctanone, cyclodecanone, cyclododecanone, cyclopentadecanone) and triethylorthoformate as reagents under classical acidic conditions.[15]

Lipophilicity of each synthetic derivative was investigated: log *P*, Parachor and Amphiphilic ratios were calculated and reported showing that the calculated log *P* values increased proportionately with the number of CH_2 groups. Their stability toward acidic conditions was also described. Toxicity using a MTT assay was also evaluated, highlighting that large-ring ketals (12C, n=11) **16f** were highly toxic.

A similar synthetic approach was previously used to investigate the formation of self-assemblies resulting from interactions of complementary ketal based Adenosine and Uridine nucleoside lipids.[16] Interestingly mixing complementary ketal based nucleosides provided new stable supramolecular systems due to complementary Adenosine-Uridine recognition.[17]

These results validated that self-assemblies could be driven *via* molecular recognition events between nucleoside lipids, which is a fundamental concept in supramolecular chemistry. These fundamental results are likely to be of interest for programmable supramolecular engineering.

2.1.2. Approach toward nucleobase-substituted nucleolipids

Mitsunobu approach to afford anchorage at N-3 position of 5-fluorouridine.

In 2013, Rosenmeyer *and coll.* reported the synthesis of nucleoterpenes in which 5-fluorouridine was substituted at *N*-3 position by either phytol or nerol using a Mitsunobu reaction **(Figure 10)**.[18] 5-fluorouridine **15** was first protected at 2',3'-OH positions by reaction with heptan-4-one in presence of triethylorthoformate under classical acidic conditions to provide a stable ketal derivative **16**. 5'-OH position was then typically protected with a (4-methoxyphenyl)diphenylmethyl (MMTs) moiety and the resulting compound was submitted to Mitsunobu reaction with either phytol or nerol (PPh_3, DEAD diethylazodicarboxylate in THF) to provide NLs in 49% average yield over 3 steps.

Resulting NLs were transformed into corresponding 5'-phosphoramidite compounds **17a-b** to provide oligonucleotides bearing a terminal phytol-alkylated 5-fluorouridine tags for further studies.

Nucleoterpenes of Thymidine and 2'-deoxyinosine.

To date, only one natural meronucleoterpene was reported (avinosol), isolated from the sponge *Dysidea* sp.. Its structure is based on a *N*-1 alkylated 2'-deoxyinosine derivative bearing a sesquiterpene residue and was found to exhibit anti-angiogenic and antimetastatic properties. Seeking inspiration in such a structure, Rosenmeyer *and coll*. reported in 2013 the first synthesis of biomimetic nucleoterpenes of Thymidine and 2'-deoxyinosine **(Figure**

11).[19] Indeed, Thymidine and 2'-deoxyinosine were easily *N*-alkylated using K_2CO_3 in DMF and alternatively geranylbromide and farnesylbromide to provide the *N*-alkylated derivatives **18a-b**, **19a-b** which were subsequently converted into corresponding 3'-*O*-phosphoramidites. These phosphoramidites were used to prepare lipophilized oligonucleotides dodecamers which were then inserted into artificial membranes (1-palmitoyl-2-oleyl-glycero-3-phos-phoethanolamine POPE and POPC).

Following a similar synthetic pathway, the authors also reported the synthesis of *N*-3 alkylated 2',3'-*O*-ethyl levulinate derivatives and corresponding acids from 5-fluorouridine **20a-b (Figure 12A)**.[20] Farnesylated NLs were then coupled to various chitosans (different sources and molecular weight) to provide covalent immobilization in homogeneous solution and also on chitosan foils. ATTO-488 was also covalently linked to the polymer as fluorescent dye and the degradation of the 5-fluorouridine bound polymer under the action of chitosanane enzyme was investigated. **Figure 12B** displays the absorbance of the acceptor-cell content of the *Franz* diffusion cell. After a total degradation time of 240h, the end of the reaction was indicated by the same measured absorbance at 268nm in both compartments of the diffusion cell (268nm being the characteristic wavelength for Uridine absorption).

The purpose was to study the potential of such polymers as biomedical material for a sustained release of a cancerostatic drug (5-fluorouridine) and also in the topical treatment of dermatological affections by taking advantage of chitosan biocompatibility with human skin.

Cytotoxic and cytostatic activities of 5-fluorouridine derivatives **20a-b** and **21** towards three carninoma cell lines -colon 5 (HT-29), hepatocellular (HepG2) and renal (RENCA) were also investigated by the same authors.[21] Indeed, if 5-fluorouridine efficiency is well known for chemotherapy against various cancers, it is very fast metabolized in the liver. Then the use of structurally modified derivatives and particularly lipophilic derivatives should be an interesting tool to investigate new modes of drug administration. Concerning HT-29 human

cells, after treatment for 48h, **20b** (R=Et) and **21** were found to exhibit significant inhibitions of the survival at 80µM compared to 5-fluorouridine. At the same concentration and concerning HePG2 cells, **20b** and **21** were shown to be 3.7 and 2.5 fold respectively more efficient than 5-fluorouridine reference. **20b** also exhibited significant better activity against murine RENCA cell line than the reference 5-fluorouridine. Cytotoxic effects of both compounds on the viability of PMA (phorbol myristate acetate)-differentiated human THP-1 macrophages were investigated as in vitro model to make a distinction between anticancer and side-effects. If **21** probed to increase significantly the cytotoxicity, **20b** was found to increase the viability compared to 5-fluorouridine. This study is rather encouraging for the use of lipophilic nucleosides as antitumor agents.

Farnesylated NLs derivatives (and **20b** R=Et in particular) were labeled with the coumarine fluorophore ATTO-425® to follow their potential incorporation and intracellular localization.[22] These compounds were also tested as cytostatic/cytotoxic agents using HT-29 human colon carcinoma cells, in comparison to 5-fluorouracil and 5-fluorouridine.

In 2011, Srivatsan *and coll.* reported the synthesis of fluorescent pyrimidine ribonucleoside analogue **22** bearing benzofuran onto the 5-position of Uracil **(Figure 13A)**.[23] For all the compounds described, the synthetic pathway involved a Stille pallado-catalyzed cross-coupling approach between commercially available 5-iodouridine and a stannane derivative. Time-resolved fluorescence spectroscopic analyses were performed to investigate the effect of solvent polarity on the excited-state decay kinetics of **22 (Figure 13B)**. In water, the benzofurane derivative exhibited the highest lifetime of 2.55 ns. This ability to respond to polarity changes and also its spectral domain of emission made it a good candidate as a fluorescent probe to study nucleic acid structures. So the 5-(benzofuran-2yl)pyrimidine analog **22** was subsequently converted into the corresponding triphosphate derivative **23 (Figure 13A)** which was efficiently incorporated into oligoribonucleotide by T7 RNA polymerase

affording fluorescent oligoribonucleotide objects. Spectroscopic studies of these oligonucleotides established that the chromophore on the ribonucleoside monomer interacted with neighbor bases involving subtle changes in its environment and then photophysical response to these changes. It was highlighted that after incorporation into an oligomer, the emissive ribonucleoside preferably indicated DNA abasic site with an increase of fluorescence intensity.

At the same time and using the same synthetic pathway, the authors reported the synthesis, characterization and the use of an Uridine nucleoside thiophene analogue[24] and its desoxyuridine analogue.

The same approach was used very recently to provide NLs hybrids incorporating emissive nucleoside following very classical coupling reaction conditions with a variety of lipidic chains before the Stille reaction step **(Figure 14A)**.[25] Fluorescent derivatives were shown to exhibit a good gelation ability in organic solvents, then the influence of self-assembling onto the photophysical behavior of these NLs was investigated. Four of these NLs provided easily organogels and it is interesting to notice that contrarily to most of the previously described low molecular weight gelators, these compounds exhibited enhanced emission upon self-organization **(Figure 14B)**. NLs **25b** and **26b** containing myristoyl chains self-assembled into nanotubes whereas **25c** and **26c** containing palmitoyl acyl chains provided twisted ribbons and fibers organization.

It was highlighted that the gelation of these hybrid materials was made reversible by external stimuli such as temperature, ultrasounds or chemicals promising interesting potential applications in the field of optical materials or probes.

2.2. Nucleotide lipids

Among non-viral vectors for therapeutic acid nucleic delivery, supramolecular assemblies of amphiphiles molecules have emerged as interesting alternative tools. In particular, nucleotide lipids taking full advantage of selective interactions between nucleic bases of both partners (NLs and nucleic acids) are prime non-toxic candidates. Two main nucleotide lipid families have been investigated; including phosphate groups attached to either 3' or 5' positions of the ribose moiety **(Figure 1)**.

2.2.1. 5'-phosphate nucleotide lipids

Regarding 5'-phosphate derivatives, Berti *and coll.* reported in 2012 the formation of NL-based anionic liposomes from POP-Ade:POPC (1-palmitoyl-2-oleoyl-phosphatidyladenosine and 1-palmitoyl-2-oleoyl-phosphatidylcholine respectively) and their association with single-stranded and double-stranded nucleic acids.[26] Interestingly, the authors demonstrated that specific interactions occurring between nucleotide lipids and single strand oligonucleotide allowed the formation of hybrid complexes, while no association was observed in the case of lipid samples POPG (1-palmitoyl-2-oleoyl-*sn*-phosphatidyl-glycerol). These types of cooperative interactions driven by molecular recognition were previously observed both in solution[27] and in low water content regime[28]. More recently, the same authors reported the ability of NLs bilayers to selectively bind single-stranded nucleic acids.[29] In another study, the binding between nucleotide lipid/dendrimer surfaces and oligonucleotide was reported.[30,31] This system featured cationic PAMAM dendrimers **(Figure 15A)**, which formed films with negatively charged nucleotide lipids. As shown in **Figure 15**, functionalized surfaces bound selectively nucleic acids depending on the type of nucleotide head group. In that example nucleotide lipids (DLPNs, **Figure 15B**) were attached to pre-adsorbed PAMAM monolayers on silica and produced layers with similar structures and composition featuring favorable nucleobases orientation. In a second step, after addition of nucleic acid, selective interactions with nucleic acids through base stacking and specific base

pairing could occur **(Figure 15C)**. According to the authors, this type of functionalized surfaces can find applications in the field of bioanalytic devices or as new drugs delivery systems.

As mentioned in the previous section, lipids nucleoside prodrugs feature important anticancer activities. Similarly, nucleotide analogs have been recently investigated as antitumor conjugates. In order to address drawbacks such as low bioavailability, poor pharmacokinetic properties, and toxic effects of nucleotide drugs, lipid prodrugs have been synthesized by Tsybulskaya *and coll.*.[32] Lipid conjugates of anticancer nucleoside clofarabine [2-chloro-9-(2-deoxy-2-fluoro-β-D-arabinofuranosyl)adenine] with 1,2- and 1,3-diacylglycerophosphates have been prepared via the phosphoramidite method. Interestingly, nucleotide lipids conjugates exhibited cytostatic activity against HL-60, A-549, MCF-7, and HeLa tumor cell lines. More recently, Berti *and coll.* investigated the self-assembly behavior of two diastereoisomers of clofarabine dioxy-ether nucleotide lipids.[33] The authors demonstrated that these derivatives showed a diastereo selective self-assembly effect, which would play a role in the different diastereoisomers bioavailabilities.

At the fundamental level, nucleotide lipids have been studied as part of protocell models. Vesicles coming from supramolecular self-assembling of NLs could be considered as pre-biotic component or cells precursors. Recently, Herdewijn *and coll.* reported series of α/β-hydroxy fatty acids and α-amino fatty acids, covalently bound to nucleoside-5-monophosphates.[34] The authors demonstrated the potential of these compounds to spontaneously self-assemble into spherical aggregates. The ability of these compounds to act as activated or reactive monomers for the “spontaneous” synthesis of oligonucleotides in abiotic conditions was investigated. An NMR study revealed that phosphoesters were cleaved between sugar and phosphate, however no oligomerization of nucleotides was observed,

indicating that these α-hydroxy or α-amino nucleotide lipids could not induce the formation of phosphodiester linkages.

2.2.2. 3'-phosphate nucleotide lipids

The modulation of the nucleobase structure, in particular the spatial orientation of nucleobases relative to the chain can have an impact on the aggregation properties of nucleotide lipids. Barthélémy *and coll.* have been working on a series of 3'-nucleotide lipid analogues, including monoalkyl phosphate,[35,36] 1,2-diacyl-*sn*-glycerol derivatives[37] as lipid moiety with a phosphate group attached to the 3'-secondary hydroxyl. Also, nucleotide-3'-monophosphate bolaamphiphile structures have been previously reported by Shimizu *and coll.*.[38]

Regarding colloidal properties, 1,2-diacyl-*sn*-glycerol derivatives have been investigated in different conditions **(Figure 16A)**, including at the air-water interface of Langmuir films,[39] vesicular systems,[40] or gels[41]. A study of Langmuir isotherms realized in 2012 revealed the formation of a quasi-hexagonal packing of bilayer domains at a low compression rate, an unexpected behavior for lipids at the air-water interface which was not previously reported for regular phospholipids **(Figure 16B)**. This observation indicated that the 3'phosphate-nucleotide polar head impacted on supramolecular assemblies. Dispersions of **27 b-c** in HEPES buffer led to the stabilization of unilamellar vesicles whereas multilamellar vesicles were observed in the same conditions for amino acid nucleotide lipid conjugates **27 b'-c' (Figure 16C)**. The different behaviors observed could be explained by the additional interactions between bilayers in the case of amino acid conjugates. Recently, hydrogels resulting from the self-assembly of DiC_{16}-3'-dT **27a** in the presence of particular counter ions (Li^+, Na^+ and K^+) were reported by Barthélémy's group **(Figure 16D)**.[41] These biocompatible soft scaffolds that exhibits elastic, thixotropic, and thermal reversibility properties were investigated for drug delivery applications.

Self-assembly properties of NLs interacting via specific interactions with oligonucleotides have long been studied in different systems and combinations.[42] In order to improve these interactions, locked nucleic acid (LNA)-based nucleotide lipids featuring 3'-monophosphate Thymidine or Adenosine[43] head groups covalently attached to 1,2-dipalmitoyl-*sn*-glycerol (DiC_{16}-3'-LNA-T and DiC_{16}-3'-LNA-A, respectively) were synthesized. As expected, LNA Adenosine lipid exhibited a high binding affinity for polyUridine with the formation of a stable complex (Kd≈43nM). In theory, such a strategy involving specific interactions can be used for novel therapeutic strategies (nucleotide lipid as RNA-binders), for example.

1,2-diacyl-*sn*-glycerol nucleotide lipids have been used for several biomedical applications **(Figure 17)**. For example, in the field of drug delivery, these molecules allow the efficient encapsulation and delivery of cisplatin. It was demonstrated that nucleoside polar heads guided the aggregates self-assembly into highly loaded and stable nanoparticles such as those shown in **Figure 17B**. Interestingly, nucleotide based nanoparticles were efficient vehicles for the delivery of cisplatin into different sensitive and resistant cancer cell lines.[44] In another contribution, nucleotide-lipids were used to stabilize solid lipid nanoparticles (SLNs) loaded with iron oxide particles and therapeutic agents **(Figure 17C)**.[45] It was demonstrated that nucleotide lipid based SLNs featured high relaxivity properties, indicating that SLNs are suitable for image-guided therapy. As seen above, **27a** self-assembled into ribbon like supramolecular structures stabilizing low molecular weight hydrogels **(Figure 17D)**. Thanks to its thixotropy properties, this bioinspired supramolecular material was injected *in vivo* to form in situ a hydrogel allowing a sustained release of small drug and protein for more than a week.[41] Such injectable non-polymeric materials represent a promising option to address several key challenges for in vivo sustained release of drugs or biologics, or as biocompatible 3D matrix for stem cells growth, for example.

Thus, NLs materials potential (under different supramolecular formats as nanoparticles, vesicles, surfaces, complexes, hydrogels) in biomedical applications, including drug delivery, tissue engineering, biomaterials may have yet to be realized, and there are many areas ripe for investigation.

3. Glyconucleolipids

As its name implies, a glyconucleolipid (GNL) results from the covalent association of a lipid, a nucleoside and a sugar. Such synthetic bioinspired hybrid amphiphiles were first reported in the literature in 2005 **(Figure 18)**.[46] This original molecular structure designed by Barthélémy *and coll.*, was a glycosyl dicarbamate Uridine **28** obtained in four steps from 5'-dimethoxytrityluridine **(Figure 18A)**. This very first synthesis involved cumbersome reactions requiring anhydrous conditions to give intermediates in moderate yields (from 36 to 55% according the three first steps). The authors have demonstrated that these glyconucleoside-based amphiphilic structures could complex DNA and form stable nucleic acids supramolecular assemblies. Hyperchromicity of a complex polyAdenosine-polyUridine (polyA-polyU) depending on temperature was evaluated in presence of increasing amounts of GNL (above the critical aggregation concentration, **Figure 18B)**. A positive shift of thermal denaturation (up to 3.5°C with ten equivalents) with an increasing amount of GNL could be demonstrated. This suggested a stabilization of the double helix resulting from DNA interactions with GNL aggregates. ^{31}P NMR experiments showed that phosphate anions complexation by glucose moieties was only achieved which GNL, indicating that both amphiphilic structure and glucose were needed to form this complex. Thus, Fourier transform infrared spectroscopy (FTIR) analyses of polyA-polyU with and without GNL revealed that nucleobase moieties were also involved via Hoogsteen or reverse Hoogsteen nucleobase

pairing with Uracil. The whole GNL structure was then involved in DNA complexation and stabilization according to a molecular model as represented in **Figure 18C**.

Barthélémy's group dealt into GNL systems in depth and developed an exclusive and extensive expertise regarding synthesis and physico-chemical properties of these particular structures. Later, more complex GNLs in which units are linked to each other by triazole moieties were designed using a copper catalyzed azide-alkyne cycloaddition (CuAAC).[47] This "click chemistry" is indeed more user-friendly and biocompatible than former chemical reactions. Over the years, a series of GNLs have been synthesized with various chemical structures according to the nucleobase (Thymidine, Uridine), the lipidic (single or double chain, fluorocarbon chain, etc.) and the sugar (glucose, galactose, lactose) moieties.[48–53] Different GNL topologies were also considered. Indeed, the sugar moiety was either linked to the nucleobase or the ribose OH-3' position, allowing in this latter case potential base pairing ability.[54] However, this review will focus only on first Thymidine-based GNLs featuring a hydrophobic chain on the 5'-ribose position **(Figure 19A)** and then on the more recently designed glyconucleoside bolaamphiphile (GNBA)[55,56] **(Figure 19B)**.

In 2009, Barthélémy *and coll.* designed a Thymidine-based GNL bearing a fluorocarbon chain called glycosyl nucleoside fluorolipid or GNF using a double "click chemistry" strategy **(Figure 20)**.[52] After azidation on Thymidine 5' position using classical conditions,[57] compound **29** was submitted to the first click reaction allowing then to form the corresponding NL **30** in 64% yield. Finally, *N*-3 alkylation of Thymidine with propargyl bromide provided the desired GNF **31** by means of a second click reaction with the suitable azido sugar.

Due to its amphiphilic structure, GNF exhibited interesting supramolecular assembly properties in solvents, allowing in particular hydrogel formation thanks to intermolecular weak interactions as hydrogen bonding and π-π stacking and hydrophobic effects. This

gelation phenomenon attested promising results in several applications from tissue engineering to nanoparticles decontamination presented below.

Chassande *and coll.* demonstrated in 2012 that GNF-based hydrogel could be used as scaffold for bone tissue engineering **(Figure 21)**.[58] They described the formation of a hydrogel at 1.5% w/v in phosphate buffer saline (PBS) and its behavior towards cells and tissues. Rheological properties were fully compatible with cells culture since gelification occurred within 20 minutes at 37°C after heating at 65°C. The system also showed characteristics of a weak hydrogel with an elastic modulus G' superior to the loss modulus G'' **(Figure 21A)**. The authors have demonstrated the hydrogel cytocompatibility regarding its excellent results on adipose stroma cells (ASCs) metabolic activity (MTT assays, not shown here) and viability after 72 hours (red neutral assays, **Figure 21B**). Thus, thanks to its rheological properties, the material was injected subcutaneously in mice under its liquid state via a syringe and reached its gel form in a few minutes at the injection area. After 60 days, a fibrous tissue containing blood vessels had invaded the hydrogel, confirming the creation of a vascularized microenvironment **(Figure 21C)**. Even if the system was non-compatible with isolated ASCs culture, it supported the survival of ASCs aggregates and even promoted *in vivo* the differentiation of ASCs into functional osteoblasts without any osteogenic factors. These experiments highlighted GNF-based hydrogel as a promising tool for bone tissue engineering.

In 2014, Barthélémy's team reported the potential of GNF-based hydrogel as a trapping scaffold for nanoparticles decontamination **(Figure 22A)**.[59] For this purpose, a 0.1% w/v hydrogel was initially prepared with an aqueous phase contaminated with positively charged nanoparticles as gold nanoparticles (AuNPs) or quantum dots (QDs) and negatively charged nanoparticles like titanium dioxide (TiO_2-NPs). After 2 to 48 hours of incubation, two phases were observed in the sample i.e. a decontaminated supernatant and a hydrogel

with entrapped nanoparticles. An example of QDs decontamination is displayed in **Figure 22** first in visible **(Figure 22B)**, then under UV light **(Figure 22C)** and finally on a nanometric scale by TEM **(Figure 22D)**. These experiments clearly showed that nanoparticles initially present in the contaminated aqueous phase could be trapped in the GNF-based hydrogel, leaving the supernatant free of contaminants. These surprising decontamination properties could be explained by a thermodynamically favorable evolution of the system due to nanoparticles interactions with supramolecular self-assembly.

In 2017, GNF was used to design a gold electrode coated by the hydrogel giving rise to a hybrid implantable macroporous device **(Figure 23A)**.[60] A coating around 1-2µm as evidenced by electron microscopy studies (SEM) and fluorescence experiments was performed by simply dipping the electrode for a few hours in a 1% w/v GNF-based hydrogel, **(Figure 23B)**. This coating did not hinder the electrochemical behavior of the electrode considering the low difference between cyclic voltammograms with and without the hydrogel **(Figure 23C)**. The presence of GNF-based hydrogel as a coating, combined with its excellent biocompatibility, constitutes a good candidate for implantable electrochemical devices.

Considering the high interest of such innovative structures, Barthélémy's group synthetized in 2011 a new GNL structure for drug delivery applications **(Figure 24)**.[53] Following the same double click chemistry approach, a Thymidine-based GNL bearing a double lipid chain **32** was synthesized **(Figure 24A)**. In contrast to its GNF homolog, **32** did not induce the formation of hydrogel but provided liposome-like structures in presence of lecithin **(Figure 24B)**. The authors hypothesized that these structures display their carbohydrate moieties at the liposome outer surface allowing potential interaction with cell membranes **(Figure 24C)**. For this, DIL (1,1'-dioctadecyl-3,3,3',3'-tetramethyl-indocarbocyanineperchlorate)-labeled liposomes were incubated with ASCs for 48 hours. Confocal microscopy showed that only formulations containing GNLs were scattered into the

cytoplasm, proving that these structures allowed interactions with cells membrane and favored their internalization **(Figure 24D)**. In parallel, liposome-like formulations containing a glyco-lipid (GL) counterpart were poorly internalized into ASCs, showing that the nucleoside also played a crucial role in this process. This could be explained by the high contribution of this moiety in terms of weak interactions as hydrogen bonding or π-π stacking. This study clearly showed that these structures are fully suitable for cell-targeting systems.

The same year, Lindhorst *and coll.* designed glycothymidines as in situ photoswitchable compounds to study structural changes (orientation, accessibility) of surface-exposed carbohydrates within the glycocalyx **(Figure 25)**.[61] For this purpose, amphiphilic glycothymidines bearing a sugar at the *N*-3 position and an alkyl chain at the secondary alcohol 5' position were synthesized following a six steps-sequence **(Figure 25A up)**. **33** was submitted to a photochemical [2+2] cycloaddition under UV light (295nm), providing dimers **34 (Figure 25A down)** whose structures were evidenced by changes in UV spectra and anomeric ribose H1' peaks shifts in ^{1}H NMR. To perform *in situ* photodimerisation into a synthetic in vivo glycosylated cell surface model, the authors used SDS micelles in which amphiphilic glycothymidines were incorporated as monomers. Calculation of diffusion constants by pulsed field gradient (PGG) ^{1}H NMR experiments allowed to demonstrated the properly incorporation of **33** into SDS micelles (diffusion constants were smaller than pure glycothymidine and SDS solution). To go further, the authors investigated sugar orientation of **33** at the surface by performing relaxation broadening titrations with Mn^{2+}-EDTA solution. Adding this latter to the system coupled with COSY ^{1}H-^{1}H NMR led to a partial cross peaks broadening of sugar groups while signals corresponding to alkyl chains were not affected **(Figure 25B)**. This proved that sugar moieties were surface-exposed and alkyl chains embedded into SDS micelles. In situ photodimerisation could be successfully achieved in a supramolecular model and demonstrated due to the appearance of multiple characteristic

anomeric ribose protons H1'. In situ [2+2] cycloaddition of these glycomimetics into a glycocalyx model altered the pattern of surface exposed carbohydrates, providing then first insights on the role of conformational control in glycobiology.

More recently, Barhtélémy's group designed a new GNL structure called GNBA for glyconucleoside bolaamphiphile, which gathers two glyconucleoside units (polar heads) linked by a lipidic chain (hydrophobic tail). The synthetic route, using double "click chemistry" again, is strictly identical to the regular GNL synthesis. In order to form this specific bola form, the last click reaction step involves two equivalents of **35** for one equivalent of di-acetylenic lipid moiety **(Figure 26)**.[52,55]

Very interestingly, bola compound **36** allowed the formation of a low molecular weight hydrogel at 1.5% w/v **(Figure 27A)**. TEM images revealed the presence of a dense anisotropic fibrillar network **(Figure 27B)**, different from GNF-based hydrogel **31** where a less connected network was observed. Thus, GNBA-based hydrogel displayed improved rheological properties compared to GNF-based hydrogel. At a fixed angular frequency of 1 $rad.s^{-1}$, its G' was almost twenty times higher than GNF-based hydrogel G' at the same molar concentration (30000Pa and 1700Pa respectively). This enhanced stiffness had a direct effect on cells development as it could promoted mechanotransduction (conversion of a mechanical stimulus into electrochemical activity), unreachable for GNF because of low G' value and yet required for tissue engineering. For biomedical purposes, injectable systems are a high-valuable advantage, avoiding thereby implantation. GNBA-based hydrogel **36** showed thixotropic properties measured by rheology through several cycles of high and low strains **(Figure 27C)**. In low strain period (within the linear viscoelastic (LVR) region of the material), G' was higher than G'' indicating the solid behavior of the hydrogel. When a high strain was applied (beyond its LVR region), G' fell below G'' leading to the collapse of the hydrogel and its liquefaction under stress. When the strain returned within its LVR region, the

material went back to its initial gel state in few minutes while keeping its rheological properties intact. This has been put into practice by a subcutaneous injection on mouse. Two hours after injection, a biopsy showed the presence of the hydrogel (ovoid shape) at the injection area, proving its injectability. GNBA-based hydrogel also displayed cytocompatibility and non-cytotoxicity with ASCs cells evaluated by MTT assays **(Figure 27D)**. In contrast to GNF **31**, GNBA-based hydrogel **36** allowed isolated stem cells culture. A 3% w/v hydrogel was incubated with stem cells and one week later, confocal microscopy coupled to live/dead viability assays were performed. Cell adhesion was evidenced regarding fibroblastoid phenotype on almost all cells and also some cell divisions occured **(Figure 27E)**. This result was correlated with enhanced rheological properties displayed by GNBA versus GNF. All these experiments point out the control of stem cells behavior by low molecular weight hydrogel architectures and the use of GNBA-based hydrogel as an extracellular matrix substitute.

4. Responsive materials

Interest in responsive materials has continued over several decades, and many investigations have been dedicated to develop sensitive molecules or macromolecules that can be inserted into smart materials or devices. The vast majority of publications describes stimuli-responsive polymers[62] that are sensitive to different stimuli, including changes in pH,[63,64] light,[65,66] redox,[67,68] enzymes,[69] salts concentration, temperature,[70] ultrasounds,[71] and electro[72] or magnetic[73] stimulations. In parallel, supramolecular systems[74] are emerging as a clear opportunity in biomedical fields thanks to their specificity and ability to respond to stimuli found in living systems. In this section, we will highlight recent results and future trends that exploit NLs and GNLs. It is our goal to emphasize these non-polymeric molecules so that

novel applications and new generations of smart materials can be realized. Constructing biomaterials using supramolecular principles *via* bottom-up approach enables molecular modulation of chemical, mechanical, and biological properties. Interestingly, the dynamic character of supramolecular interactions provides systems that can respond to specific stimuli through a fundamental change in material properties. The ability to accurately control structure, bioactivity, and mechanical properties using a variety of biologically compatible triggers represent an obvious option for controlling the delivery of therapeutics or drugs. Depending on applications, reversible or irreversible switches may be envisioned. As shown in **Figure 28**, two types of stimuli, including external (temperature, ultrasounds, light, magnetic field, mechanical stress, etc) or internal (pH, specific, molecular interactions, enzymes, salts, ionic strength, redox potential, etc) applied triggers may be developed in the case supramolecular systems. Regarding drug delivery applications, both internal and external stimuli have been investigated in the case of NLs and GNLs, particularly redox, pH, salts concentration and mechanical stress (**Figure 28** gray frames).

4.1. Internal or environmental stimuli

Internal stimuli, which correspond to local or environmental changes in terms of pH, ionic strength, or redox potential, are also common triggers used for the release of active principle ingredients (APIs) from supramolecular systems.[70,75] A basic principle is to induce changes in a supramolecular system upon stimulation via a selected trigger. Thus, the material undergoes a transition from an organization to another one resulting in the release of APIs.

Regarding salts concentration stimulus, Barthélémy's strategy entailed using calcium cations associated with phosphates moieties belonging to both nucleotide lipids and DNA.[37] In addition to hydrogen-bonding and base π-π stacking, such a cationic bridge between the

two species would allow the stabilization of complexes. The authors demonstrated that the anionic nucleotide lipid ($DiC_{16}dT$) was able to bind nucleic acids via DNA-nucleotide lipid interactions allowing the stabilization of DNA plasmid lipoplexes in the presence of Ca^{2+}. In order to use these lipoplexes as an alternative to cationic systems for transfection applications, the authors hypothesized that the complex stability could be tuned depending on the Ca^{2+} concentration. It was observed that the nucleotide lipid/DNA stability depended on calcium concentrations. Indeed, nucleotide lipid/DNA complexes were stable only above a concentration of 1mM, which is much higher than intracellular calcium concentration ($[Ca^{2+}]$= 1µM) indicating that lipoplexes could release DNA into cells. Results of transfection assays performed on mammalian cell lines (Hek 293 human embryo kidney) showed that anionic nucleotide lipids were more efficient compared to regular anionic phospholipids in the same conditions. This demonstrated that the nucleotide moiety influenced lipid-DNA associations and enhanced transfection efficacy of the natural anionic phospholipid.

The site-specific release of APIs represents a promising approach to address issues in drug delivery.[76] In that regard, pH-sensitive drug delivery systems have been widely investigated. For example, it is known that pH sensitive system can take advantage of acidic pH of tumor environment.[77] Also large pH shifts from neutral pH in blood to pH = 4.0–6.5 in intracellular endosomes can be used as a trigger to favor intracellular drug delivery.[78–81] pH responsive NLs were reported only recently **(Figure 29)**.[82] In this work a novel approach involving orthoester-based NLs was developed in order to control fusion properties. It was shown that orthoester modification of NLs (ONLs) resulted in the formation of pH-sensitive liposomes able to release fatty alcohols into biological membrane in acidic conditions. The presence of fatty alcohols destabilized vesicles and the formation of lamellar phases was observed **(Figure 29A, Figure 29B)**. The association of fatty alcohol with phosphocholine natural lipids (DOPC) could explain such a transition *via* a modulation of the membrane

curvature. As an example of application, a cationic ONL was used to deliver a therapeutic siRNA targeting particles a human RecQ helicase (RECQL4) over expressed in aggressive breast cancers (Luminal B).

As an alternative to pH responsiveness, several cleavable or detachable chemical systems have been investigated, including those sensitive to reducing conditions.[83,84] Indeed, tumoral extracellular microenvironment is known to be reductive due to the released of glutathione and reductases by tumor cells and the presence of redox enzymes. Within this context, a nucleoside-lipid featuring a cleavable disulfide polyethylene glycol (PEG) was synthesized in order to improve the internalization of drug carrier into tumor cells. PEGylation of nano-objects remains an important technology, in particular for the delivery of drugs *in vivo*. However, PEGylation is detrimental to cellular internalization of stealth nano-objects, due to their poor interactions with cellular membranes. An alternative is to release PEG moieties next to tumor cells in order to restore cellular internalization. Barthélémy *and coll.* reported a PEG detachable nucleotide lipid named DOU-SS-PEG2000 **(Figure 30A)**.[85] This nucleoside lipid self organized to give spontaneously micelles of 20nm in diameter. Physico-chemical studies revealed that a reduction induced a transition from micellar systems to vesicular states **(Figure 30B)**. In the case of liposome formulations with a cationic lipid (DOTAU), cleavage of PEG in reduction conditions resulted in liposomes featuring cationic surfaces **(Figure 30C)**. As a result, an enhanced cellular internalization of micelles and liposomes nano-objects in ovarian cancer cells line was observed. This demonstrates that PEG detachable nucleoside-lipid can be inserted in formulations to optimize cellular internalization efficacy for *in vivo* anticancer applications.

4.2. External stimuli

Numerous responsive drug delivery systems based on externally applied triggers such as light, temperature, ultrasounds, electric or magnetic fields, have been investigated.[86,87] With regard to mechanically responsive materials, we are currently witnessing an increasing number of reports, in particular in the context of biomedicine which highlights the relevance of dynamic mechanical properties in bioengineering[88,89] and drug delivery applications[90,91] for example. While recognizing the importance of nucleobases interactions in self-assemblies formation and in an effort to expand the synthetic mechanical responsive supramolecular toolbox, a GNL was studied by Grinstaff *and coll.* as a responsive low molecular weight gel for drug delivery application **(Figure 31)**.[92] As expected, a weak mechanical shear stimulation applied to the GNL based hydrogel previously loaded with an antibody (anti-TNFα) increased the release of this latter compared with the non-stimulated hydrogel. This demonstrates the utility of such bioinspired materials for the control release of delicate and bioactive substances.

The use of NLs or GNLs for preparing responsive supramolecular materials, which has been investigated only recently, represents a unique approach that complements previous systems based on polymers. Continued research in this field will afford novel responsive supramolecular materials (gels, nanoparticles, micro and nano emulsions) able to respond to different stimuli, including magnetic and electrical field, light, ultrasounds, enzymes or specific molecular interactions, which are still unexplored so far **(Figure 28)**. Work is currently in progress on a number of bioinspired nucleoside structures to extent the current repertoire of responsive systems.

Conclusion

Recent publications in the field of nucleic acid based amphiphiles over the past seven years open up promising avenues for the design and development of soft materials. Nature is an obvious source of inspiration and looking at the supramolecular behavior of biomolecules could help us to discover new advanced materials. The above examples illustrate how efficient supramolecular devices, biotechnological tools, drug delivery systems, therapeutic strategies and responsive materials have been devised from nucleolipids and glyconucleolipids. By examining the scientific contribution of main academic actors in the field, we have identified two areas of interest for the next decade: a) a fundamental exploration of new methods to construct soft materials (e.g., low molecular weight gels, nano-objects, responsive devices), and b) the evaluation of these supramolecular tools for biomedical and technological applications (e.g., regenerative medicine, bioprinting, drug delivery, medicinal chemistry).

Regarding the fundamental aspects of nucleolipids as supramolecular tools, one will note that Guanine and Cytosine derivatives have been poorly investigated compared to Thymine, Adenine, or Uracil structures. Interestingly, Guanine and Cytosine are known to form particular supramolecular structures in living systems. G-quadruplexes, which are formed by nucleic acids rich in Guanine, correspond to four stranded helical secondary structures located most of the time at the end of chromosomes. Such supramolecular organizations, which would be involved in important mechanisms for regulating multiple biological processes in vivo,[93] are stabilized by the presence of cations, especially potassium. Likewise, i-motifs,[94] which can be observed in nucleic acid sequences rich in cytosine, correspond to four-stranded oligonucleotide supramolecular structures. Those secondary organizations are here stabilized by acidic conditions. Thanks to their pH dependent folding, i-motifs would be of interest as pH switches for applications in nanotechnology. Hence, the properties of G-quadruplexes and i-motifs hold great potentials for the development of

sensors or switches, which could be useful for advanced biomedical applications. The synthetic access to Guanine and Cytosine nucleolipids has consistently lagged behind that of Thymine, Adenine of Uracil analogues. As a consequence, many of key supramolecular developments in the field have been limited to Thymine-Thymine, Adenine-Adenine or Thymine-Adenine systems. Extending the nucleolipids repertoire to at least the five natural nucleobases derivatives (A,T,C,G,U) would open the way toward programmable or encoded supramolecular systems and allow the construction of G-quadruplex or i-Motif responsive devices, for example.

The covalent combination of nucleic acid features with lipid provides means and tools to construct complex matters possessing emerging features that do not exist when these families are taken separately. Through the appropriate supramolecular organization of specific nucleolipids in organized patterns, they may be amenable to construct novel smart and functional materials for biomedical applications. Together with the corresponding areas in chemistry, biology, physics and technology, future researches with these hybrid biomolecules will certainly open a door to the design of both simple biocompatible devices or complex and programmable, encoded, supramolecular materials.

Acknowledgements

This work, realized within the framework of the Laboratory of Excellence AMADEus with the reference ANR-10-LABX-0042-AMADEUS, has benefitted from aid by the state operated “Agence Nationale de la Recherche" under the program “Initiative for Excellence IdEx Bordeaux” holding the reference ANR-10-IDEX-0003-02. The work has also been supported by INSERM and CNRS. Julie Baillet and Aladin Hamoud thank respectively DGA and the French MESRI for PhD grants.

Received: ((will be filled in by the editorial staff))

Revised: ((will be filled in by the editorial staff))

Published online: ((will be filled in by the editorial staff))

References

[1] H. Rosemeyer, *Chem. Biodivers.* **2005**, *2*, 977.

[2] A. Gissot, M. Camplo, M. W. Grinstaff, P. Barthélémy, *Org. Biomol. Chem.* **2008**, *6*, 1324.

[3] U. Pradere, E. C. Garnier-Amblard, S. J. Coats, F. Amblard, R. F. Schinazi, *Chem. Rev.* **2014**, *114*, 9154.

[4] B. Roy, A. Depaix, C. Périgaud, S. Peyrottes, *Chem. Rev.* **2016**, *116*, 7854.

[5] L. Simeone, G. Mangiapia, C. Irace, A. Di Pascale, A. Colonna, O. Ortona, L. De Napoli, D. Montesarchio, L. Paduano, *Mol. Biosyst.* **2011**, *7*, 3075.

[6] L. Simeone, G. Mangiapia, G. Vitiello, C. Irace, A. Colonna, O. Ortona, D. Montesarchio, L. Paduano, *Bioconjug. Chem.* **2012**, *23*, 758.

[7] S. Leijen, S. A. Burgers, P. Baas, D. Pluim, M. Tibben, E. van Werkhoven, E. Alessio, G. Sava, J. H. Beijnen, J. H. M. Schellens, *Invest. New Drugs* **2015**, *33*, 201.

[8] G. Mangiapia, G. D'Errico, L. Simeone, C. Irace, A. Radulescu, A. Di Pascale, A. Colonna, D. Montesarchio, L. Paduano, *Biomaterials* **2012**, *33*, 3770.

[9] D. Montesarchio, G. Mangiapia, G. Vitiello, D. Musumeci, C. Irace, R. Santamaria, G. D'Errico, L. Paduano, *Dalton Trans. Camb. Engl. 2003* **2013**, *42*, 16697.

[10] L. Simeone, C. Irace, A. Di Pascale, D. Ciccarelli, G. D'Errico, D. Montesarchio, *Eur. J. Med. Chem.* **2012**, *57*, 429.

[11] C. Riccardi, D. Musumeci, C. Irace, L. Paduano, D. Montesarchio, *Eur. J. Org. Chem.* **2017**, *2017*, 1100.

[12] X. Mulet, T. Kaasgaard, C. E. Conn, L. J. Waddington, D. F. Kennedy, A. Weerawardena, C. J. Drummond, *Langmuir* **2010**, *26*, 18415.

[13] O. Kaczmarek, H. A. Scheidt, A. Bunge, D. Föse, S. Karsten, A. Arbuzova, D. Huster, J. Liebscher, *Eur. J. Org. Chem.* **2010**, *2010*, 1579.

[14] A. Nuthanakanti, S. G. Srivatsan, *ACS Appl. Mater. Interfaces* **2017**, *9*, 22864.

[15] E. Malecki, H. Rosemeyer, *Helv. Chim. Acta* **2010**, *93*, 1500.

[16] L. Moreau, M. Camplo, M. Wathier, N. Taib, M. Laguerre, I. Bestel, M. W. Grinstaff, P. Barthélémy, *J. Am. Chem. Soc.* **2008**, *130*, 14454.

[17] N. Taib, A. Aimé, L. Moreau, M. Camplo, S. Houmadi, B. Desbat, M. Laguerre, M. W. Grinstaff, I. Bestel, P. Barthélémy, *J. Colloid Interface Sci.* **2012**, *377*, 122.

[18] E. Malecki, C. Knies, E. Werz, H. Rosemeyer, *Chem. Biodivers.* **2013**, *10*, 2209.

[19] K. Köstler, E. Werz, E. Malecki, M. Montilla-Martinez, H. Rosemeyer, *Chem. Biodivers.* **2013**, *10*, 39.

[20] E. Malecki, R. Viere, H. Rosemeyer, *Chem. Biodivers.* **2013**, *10*, 1828.

[21] A. Farhat, E. Malecki, G. A. Bonaterra, D. Röthlein, M. Wolf, J. Schmitt, H. Rosemeyer, R. Kinscherf, *Chem. Biodivers.* **2014**, *11*, 469.

[22] E. Malecki, A. Farhat, G. A. Bonaterra, D. Röthlein, M. Wolf, J. Schmitt, R. Kinscherf, H. Rosemeyer, *Chem. Biodivers.* **2013**, *10*, 2235.

[23] A. A. Tanpure, S. G. Srivatsan, *Chem. – Eur. J.* **2011**, *17*, 12820.

[24] M. G. Pawar, S. G. Srivatsan, *Org. Lett.* **2011**, *13*, 1114.

[25] A. Nuthanakanti, S. G. Srivatsan, *Nanoscale* **2016**, *8*, 3607.

[26] C. Montis, S. Milani, D. Berti, P. Baglioni, *J. Colloid Interface Sci.* **2012**, *373*, 57.

[27] M. Banchelli, D. Berti, P. Baglioni, *Angew. Chem. Int. Ed.* **2007**, *46*, 3070.

[28] S. Milani, F. Baldelli Bombelli, D. Berti, P. Baglioni, *J. Am. Chem. Soc.* **2007**, *129*, 11664.

[29] C. Montis, Y. Gerelli, G. Fragneto, T. Nylander, P. Baglioni, D. Berti, *Colloids Surf. B Biointerfaces* **2016**, *137*, 203.

[30] M. Y. Arteta, D. Berti, C. Montis, R. A. Campbell, L. A. Clifton, M. W. A. Skoda, O. Soltwedel, P. Baglioni, T. Nylander, *Soft Matter* **2014**, *10*, 8401.

[31] M. Y. Arteta, D. Berti, C. Montis, R. A. Campbell, C. Eriksson, L. A. Clifton, M. W. A. Skoda, O. Soltwedel, A. Koutsioubas, P. Baglioni, T. Nylander, *Soft Matter* **2015**, *11*, 1973.

[32] I. Tsybulskaya, T. Kulak, A. Baranovsky, M. Golubeva, B. Kuzmitsky, E. Kalinichenko, *Bioorg. Med. Chem.* **2013**, *21*, 5414.

[33] P. Sandin, F. B. Bombelli, B. Castroflorio, C. Müller, J. Obermeier, G. Karlsson, K. Edwards, P. Baglioni, D. Berti, *New J. Chem.* **2014**, *38*, 5247.

[34] K. L. Gangadhara, P. Srivastava, J. Rozenski, H.-P. Mattelaer, V. Leen, W. Dehaen, J. Hofkens, E. Lescrinier, P. Herdewijn, *J. Syst. Chem.* **2014**, *5*, 5.

[35] N. Campins, P. Dieudonné, M. W. Grinstaff, P. Barthélémy, *New J. Chem.* **2007**, *31*, 1928.

[36] I. Bestel, N. Campins, A. Marchenko, D. Fichou, M. W. Grinstaff, P. Barthélémy, *J. Colloid Interface Sci.* **2008**, *323*, 435.

[37] S. Khiati, N. Pierre, S. Andriamanarivo, M. W. Grinstaff, N. Arazam, F. Nallet, L. Navailles, P. Barthélémy, *Bioconjug. Chem.* **2009**, *20*, 1765.

[38] R. Iwaura, K. Yoshida, M. Masuda, K. Yase, T. Shimizu, *Chem. Mater.* **2002**, *14*, 3047.

[39] B. Desbat, N. Arazam, S. Khiati, G. Tonelli, W. Neri, P. Barthélémy, L. Navailles, *Langmuir* **2012**, *28*, 6816.

[40] G. Tonelli, K. Oumzil, F. Nallet, C. Gaillard, L. Navailles, P. Barthélémy, *Langmuir* **2013**, *29*, 5547.

[41] M. A. Ramin, K. R. Sindhu, A. Appavoo, K. Oumzil, M. W. Grinstaff, O. Chassande, P. Barthélémy, *Adv. Mater.* **2017**, *29*, 1605227.

[42] K. Sugiyasu, M. Numata, N. Fujita, S. M. Park, Y. J. Yun, B. H. Kim, S. Shinkai, *Chem. Commun.* **2004**, *0*, 1996.

[43] A. Patwa, G. Salgado, F. Dole, L. Navailles, P. Barthélémy, *Org. Biomol. Chem.* **2013**, *11*, 7108.

[44] S. Khiati, D. Luvino, K. Oumzil, B. Chauffert, M. Camplo, P. Barthélémy, *ACS Nano* **2011**, *5*, 8649.

[45] K. Oumzil, M. A. Ramin, C. Lorenzato, A. Hémadou, J. Laroche, M. J. Jacobin-Valat, S. Mornet, C.-E. Roy, T. Kauss, K. Gaudin, G. Clofent-Sanchez, P. Barthélémy, *Bioconjug. Chem.* **2016**, *27*, 569.

[46] J. Arigon, C. A. H. Prata, M. W. Grinstaff, P. Barthélémy, *Bioconjug. Chem.* **2005**, *16*, 864.

[47] H. C. Kolb, M. G. Finn, K. B. Sharpless, *Angew. Chem. Int. Ed Engl.* **2001**, *40*, 2004.

[48] L. Latxague, M.-J. Dalila, A. Patwa, S. Ziane, O. Chassande, G. Godeau, P. Barthélémy, *Comptes Rendus Chim.* **2012**, *15*, 29.

[49] M. A. Ramin, J. Baillet, S. Benizri, L. Latxague, P. Barthélémy, *New J. Chem.* **2016**, *40*, 9903.

[50] G. Godeau, J. Bernard, C. Staedel, P. Barthélémy, *Chem. Commun. Camb. Engl.* **2009**, *0* 5127.

[51] G. Godeau, P. Barthélémy, *Langmuir ACS J. Surf. Colloids* **2009**, *25*, 8447.

[52] G. Godeau, C. Brun, H. Arnion, C. Staedel, P. Barthélémy, *Tetrahedron Lett.* **2010**, *51*, 1012.

[53] L. Latxague, S. Ziane, O. Chassande, A. Patwa, M.-J. Dalila, P. Barthélémy, *Chem. Commun. Camb. Engl.* **2011**, *47*, 12598.

[54] L. Latxague, A. Patwa, E. Amigues, P. Barthélémy, *Mol. Basel Switz.* **2013**, *18*, 12241.

[55] L. Latxague, M. A. Ramin, A. Appavoo, P. Berto, M. Maisani, C. Ehret, O. Chassande, P. Barthélémy, *Angew. Chem. Int. Ed Engl.* **2015**, *54*, 4517.

[56] L. Latxague, A. Gaubert, D. Maleville, J. Baillet, M. A. Ramin, P. Barthélémy, *Gels* **2016**, *2*, 25.

[57] X. Hu, M. T. Tierney, M. W. Grinstaff, *Bioconjug. Chem.* **2002**, *13*, 83.

[58] S. Ziane, S. Schlaubitz, S. Miraux, A. Patwa, C. Lalande, I. Bilem, S. Lepreux, B. Rousseau, J.-F. Le Meins, L. Latxague, P. Barthélémy, O. Chassande, *Eur. Cell. Mater.* **2012**, *23*, 147.

[59] A. Patwa, J. Labille, J.-Y. Bottero, A. Thiéry, P. Barthélémy, *Chem. Commun.* **2015**, *51*, 2547.

[60] D. Jain, A. Karajic, M. Murawska, B. Goudeau, S. Bichon, S. Gounel, N. Mano, A. Kuhn, P. Barthélémy, *ACS Appl. Mater. Interfaces* **2017**, *9*, 1093.

[61] K. Schwekendiek, H. Kobarg, L. Daumlechner, F. D. Sönnichsen, T. K. Lindhorst, *Chem. Commun.* **2011**, *47*, 9399.

[62] D. Roy, J. N. Cambre, B. S. Sumerlin, *Prog. Polym. Sci.* **2010**, *35*, 278.

[63] W. Gao, J. M. Chan, O. C. Farokhzad, *Mol. Pharm.* **2010**, *7*, 1913.

[64] A. J. Convertine, C. Diab, M. Prieve, A. Paschal, A. S. Hoffman, P. H. Johnson, P. S. Stayton, *Biomacromolecules* **2010**, *11*, 2904.

[65] J. Jiang, X. Tong, Y. Zhao, *J. Am. Chem. Soc.* **2005**, *127*, 8290.

[66] H. Kang, A. C. Trondoli, G. Zhu, Y. Chen, Y.-J. Chang, H. Liu, Y.-F. Huang, X. Zhang, W. Tan, *ACS Nano* **2011**, *5*, 5094.

[67] J. Xu, A. Singh, M. M. Amiji, *BMC Cancer* **2014**, *14*, 75.

[68] R. Cheng, F. Feng, F. Meng, C. Deng, J. Feijen, Z. Zhong, *J. Control. Release Off. J. Control. Release Soc.* **2011**, *152*, 2.

[69] M. T. Basel, T. B. Shrestha, D. L. Troyer, S. H. Bossmann, *ACS Nano* **2011**, *5*, 2162.

[70] D. Schmaljohann, *Adv. Drug Deliv. Rev.* **2006**, *58*, 1655.

[71] S. Hernot, A. L. Klibanov, *Adv. Drug Deliv. Rev.* **2008**, *60*, 1153.

[72] J. Ge, E. Neofytou, T. J. Cahill, R. E. Beygui, R. N. Zare, *ACS Nano* **2012**, *6*, 227.

[73] R. Cheng, F. Meng, C. Deng, H.-A. Klok, Z. Zhong, *Biomaterials* **2013**, *34*, 3647.

[74] M. J. Webber, *Bioeng. Transl. Med.* **2016**, *1*, 252.

[75] S. Ganta, H. Devalapally, A. Shahiwala, M. Amiji, *J. Control. Release Off. J. Control. Release Soc.* **2008**, *126*, 187.

[76] C. S. Kim, B. Duncan, B. Creran, V. M. Rotello, *Nano Today* **2013**, *8*, 439.

[77] I. F. Tannock, D. Rotin, *Cancer Res.* **1989**, *49*, 4373.

[78] C. L. Walsh, J. Nguyen, F. C. Szoka, *Chem. Commun.* **2012**, *48*, 5575.

[79] E. Fattal, P. Couvreur, C. Dubernet, *Adv. Drug Deliv. Rev.* **2004**, *56*, 931.

[80] C. Masson, M. Garinot, N. Mignet, B. Wetzer, P. Mailhe, D. Scherman, M. Bessodes, *J. Control. Release Off. J. Control. Release Soc.* **2004**, *99*, 423.

[81] Z. Huang, X. Guo, W. Li, J. A. MacKay, F. C. Szoka, *J. Am. Chem. Soc.* **2006**, *128*, 60.

[82] K. Oumzil, S. Benizri, G. Tonelli, C. Staedel, A. Appavoo, M. Chaffanet, L. Navailles, P. Barthélémy, *ChemMedChem* **2015**, *10*, 1797.

[83] D. Kirpotin, K. Hong, N. Mullah, D. Papahadjopoulos, S. Zalipsky, *FEBS Lett.* **1996**, *388*, 115.

[84] P. Sun, D. Zhou, Z. Gan, *J. Controlled Release* **2011**, *155*, 96.

[85] K. Oumzil, S. Khiati, M. W. Grinstaff, P. Barthélémy, *J. Control. Release Off. J. Control. Release Soc.* **2011**, *151*, 123.

[86] R. Langer, *Science* **1990**, *249*, 1527.

[87] S. Mura, J. Nicolas, P. Couvreur, *Nat. Mater.* **2013**, *12*, 991.

[88] A. J. Engler, S. Sen, H. L. Sweeney, D. E. Discher, *Cell* **2006**, *126*, 677.

[89] J. H. Wen, L. G. Vincent, A. Fuhrmann, Y. S. Choi, K. C. Hribar, H. Taylor-Weiner, S. Chen, A. J. Engler, *Nat. Mater.* **2014**, *13*, 979.

[90] H. D. Lu, D. E. Soranno, C. B. Rodell, I. L. Kim, J. A. Burdick, *Adv. Healthc. Mater.* **2013**, *2*, 1028.

[91] N. Korin, M. Kanapathipillai, B. D. Matthews, M. Crescente, A. Brill, T. Mammoto, K. Ghosh, S. Jurek, S. A. Bencherif, D. Bhatta, A. U. Coskun, C. L. Feldman, D. D. Wagner, D. E. Ingber, *Science* **2012**, *337*, 738.

[92] J. A. Kaplan, P. Barthélémy, M. W. Grinstaff, *Chem. Commun.* **2016**, *52*, 5860.

[93] D. Rhodes, H. J. Lipps, *Nucleic Acids Res.* **2015**, *43*, 8627.

[94] H. A. Day, P. Pavlou, Z. A. E. Waller, *Bioorg. Med. Chem.* **2014**, *22*, 4407.

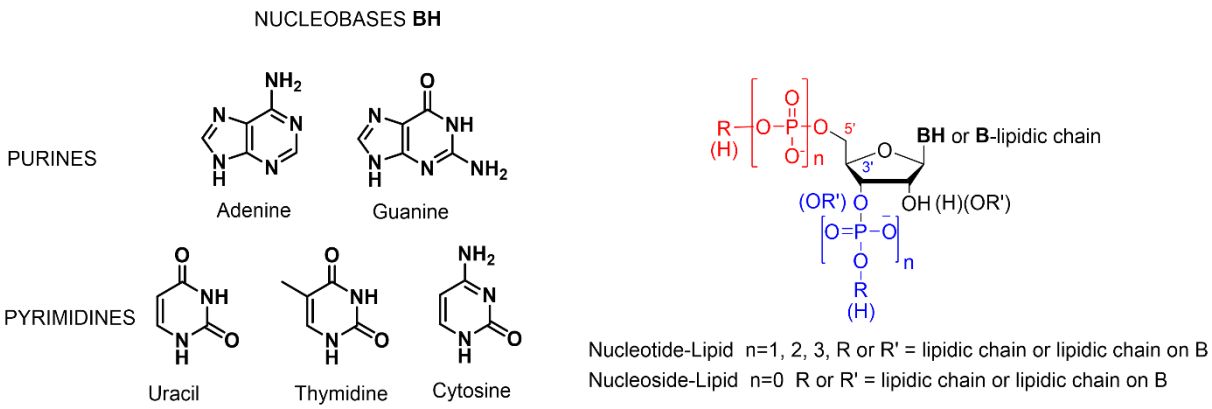

Figure 1. Right) General structure of nucleolipids showing different possible substitutions on the ribose moieties at the 2', 3' and 5' positions. Nucleotide-lipids possess a phosphate moiety, whereas nucleoside lipids are only functionalized with lipid chains. Left) Chemical structures of purine and pyrimidine natural nucleobases.

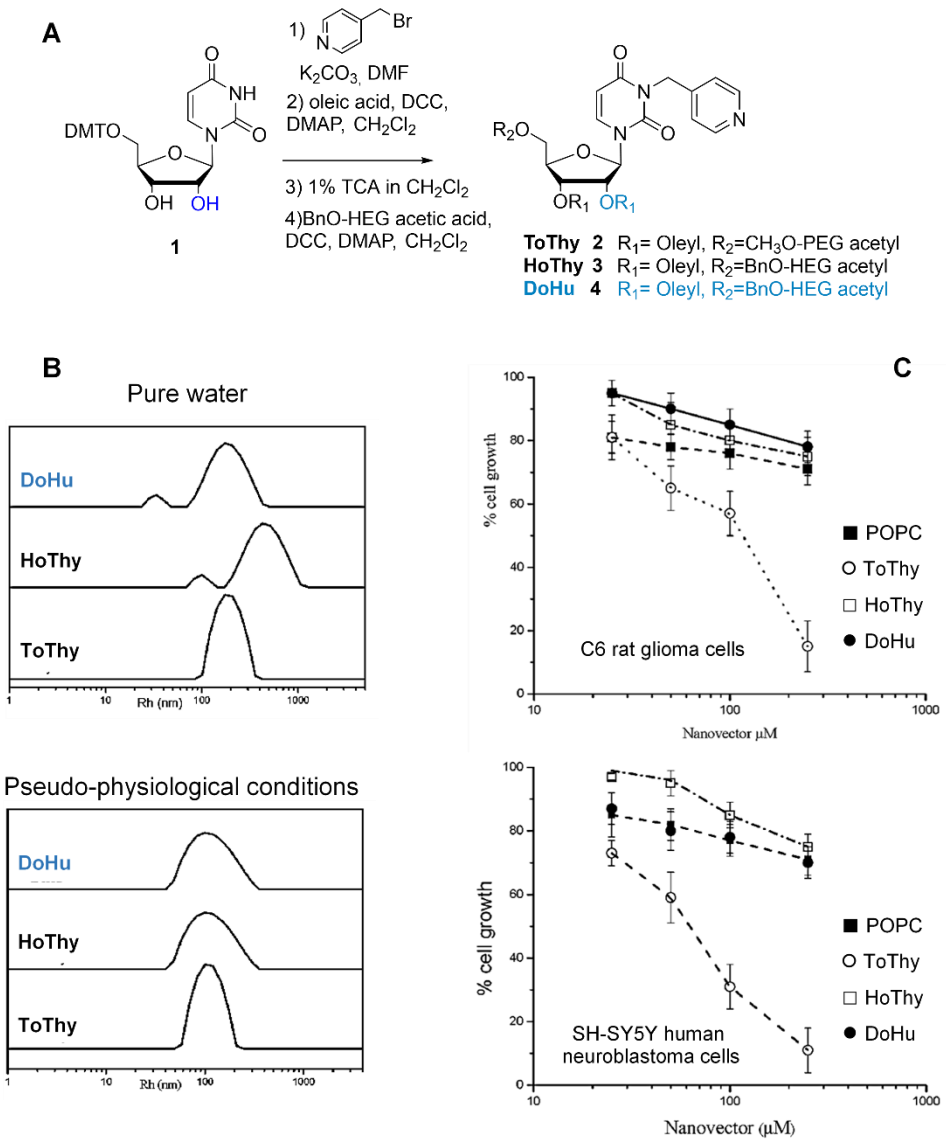

Figure 2. Nucleolipid nanovectors as molecular carrier. **A.** NLs synthetic route **B.** Hydrodynamic radii distribution at 90° of aggregates formed by NLs in both water (up) and pseudo-physiological conditions (down). Concentration of 0.2mmol.kg^{-1} for all systems. **C.** Cells viability evaluations (MTT assays) performed on indicated cell lines treated for 72h with nanovectors. Adapted from[5]

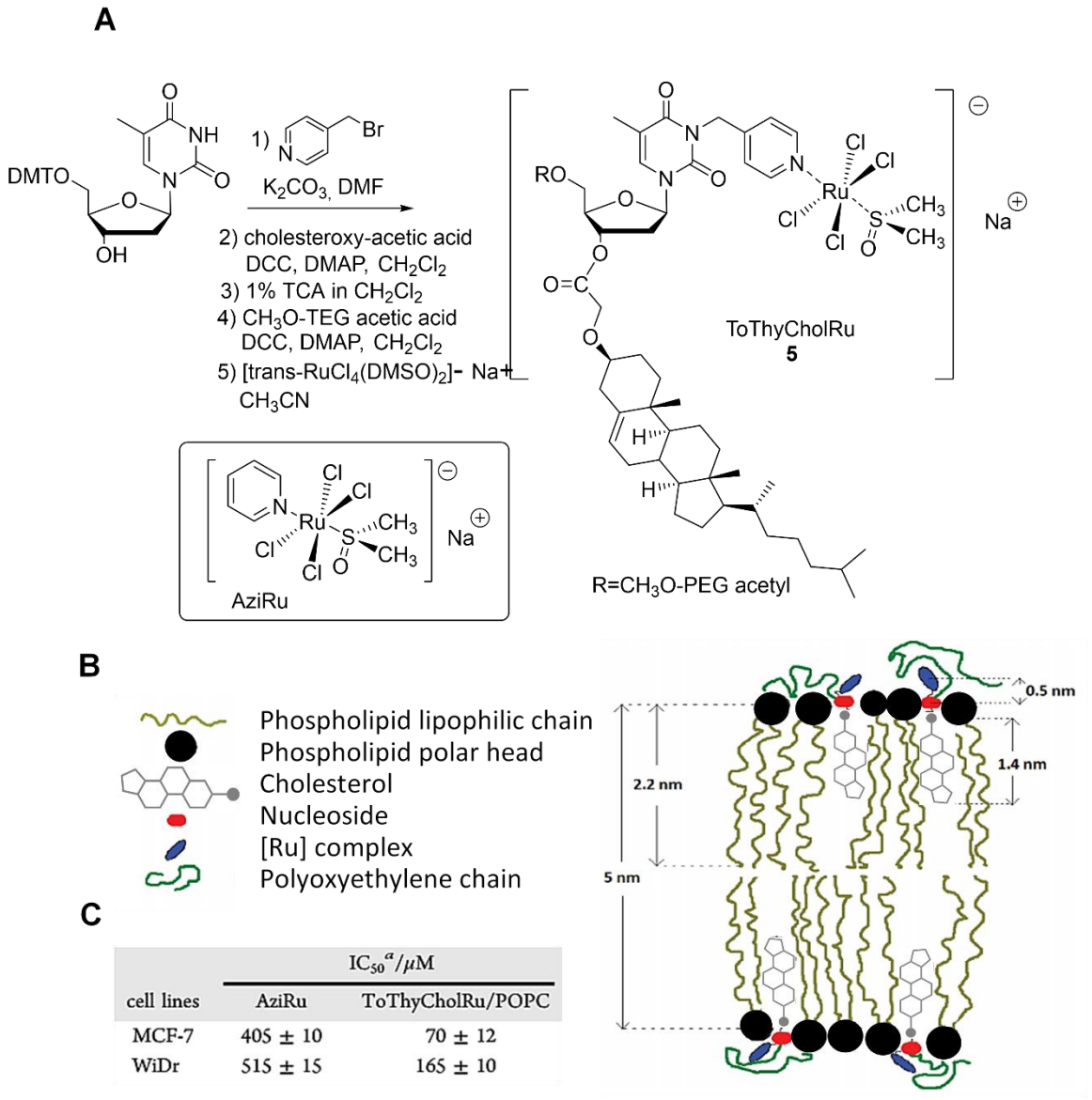

	$IC_{50}{}^{a}/\mu M$	
cell lines	AziRu	ToThyCholRu/POPC
MCF-7	405 ± 10	70 ± 12
WiDr	515 ± 15	165 ± 10

Figure 3. Cholesterol-based nucleolipid-ruthenium complex for antineoplastic therapy. **A.** Synthetic procedure for the preparation of ToThyCholRu (up) and molecular structure of pyridine-based ruthenium complex (frame). **B.** Schematic representation of ToThyCholRu lodged into a bilayer. **C.** IC_{50} values of AziRu and ToThyCholRu/POPC liposome in the indicated cell lines following 72h of incubation. Adapted from[6]

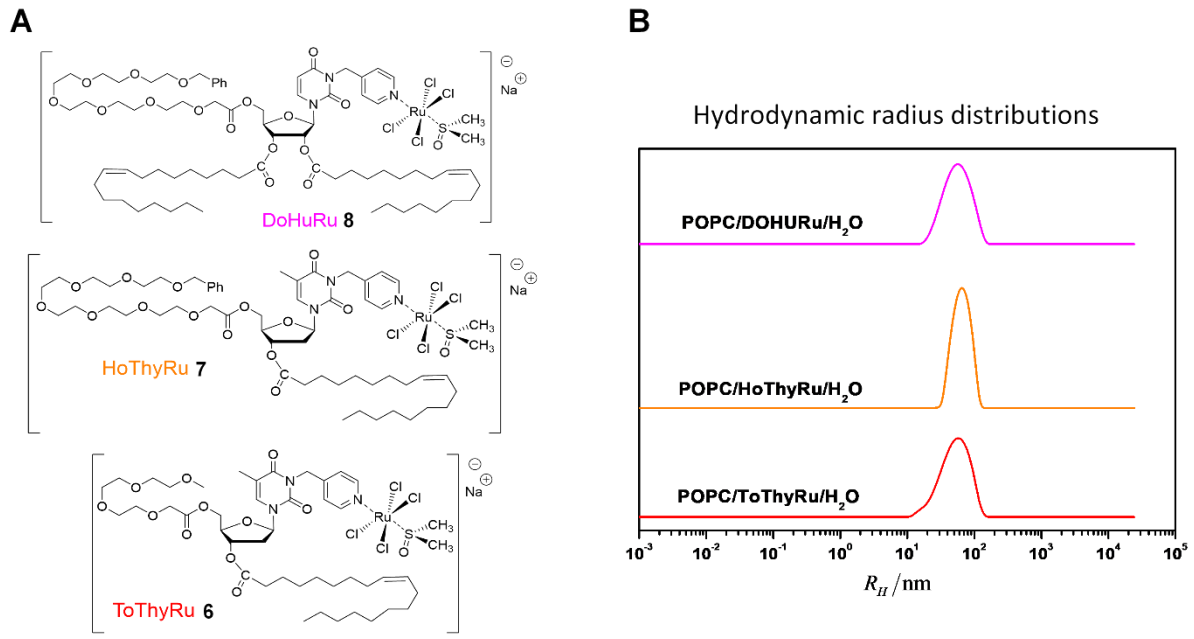

Figure 4. Ruthenium-based complex nanocarriers for cancer therapy. **A.** Chemical structures of **ToThyRu 6**, **HoThyRu 7**, and **DoHuRu 8**. **B.** Hydrodynamic radius distributions in water for ternary systems POPC/[Ru complex]/H_20 at 85/15 molar ratio between the phospholipid and 0.1mmol/kg solution of the ruthenium complex. Adapted from[8]

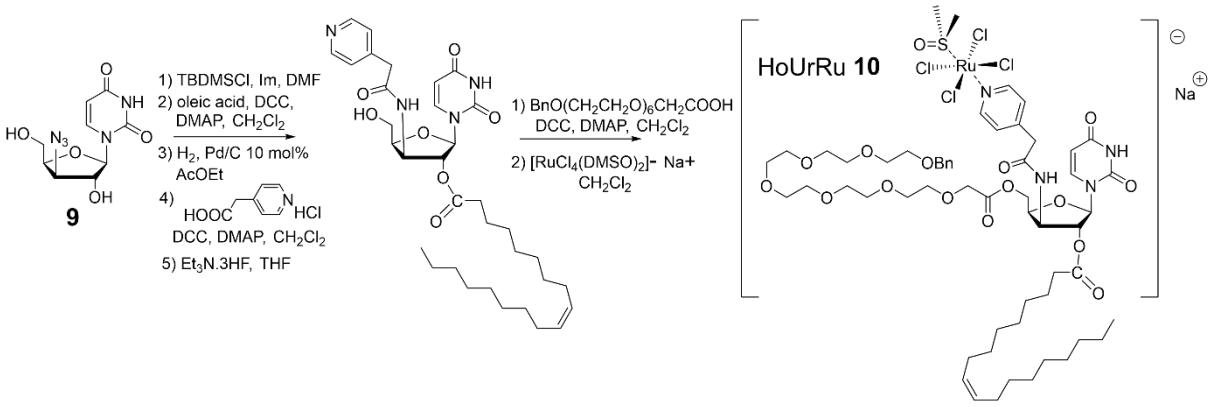

Figure 5. **HoUrRu** complex **10** synthesis. Adapted from[9]

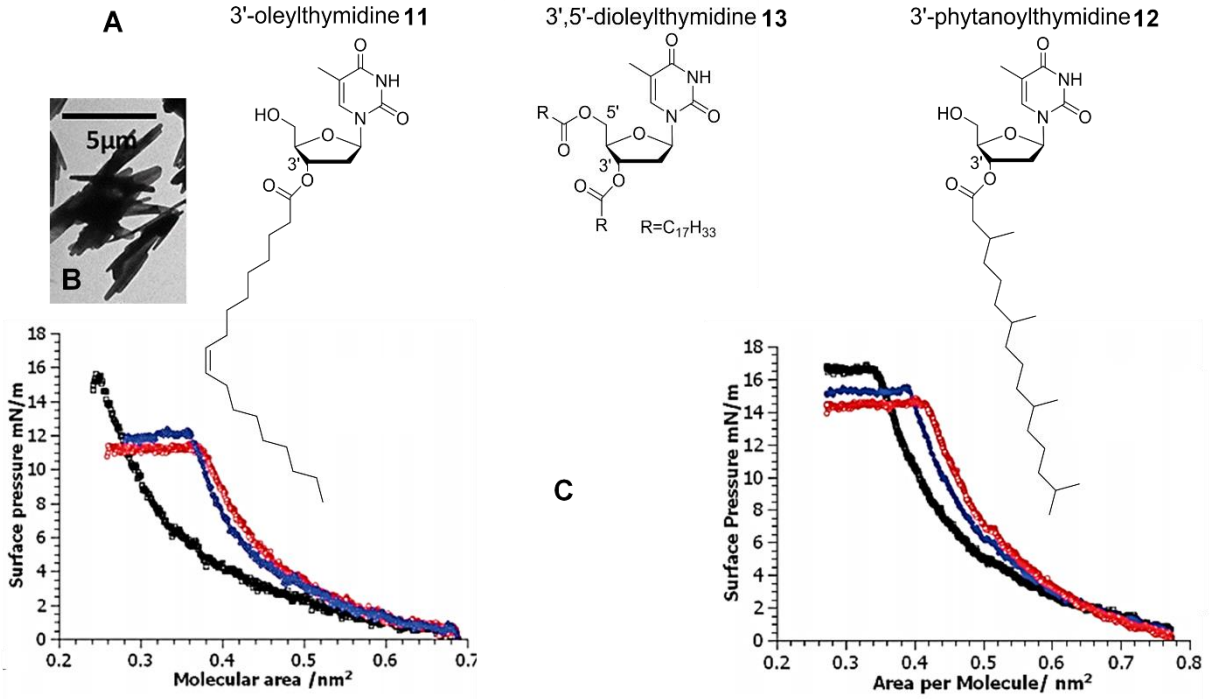

Figure 6. Nonionic Thymidine nucleolipids **11**, **12**, **13** **A.** NLs chemical structures. **B.** TEM image of spherulites from 3'-oleoylthymidine **11** (scale bar: 5µm). **C.** Surface pressure-area isotherms for monolayers of 3'-oleylthymidine **11** and 3'-phytanoylthymidine **12**. Blue curve: H_2O + 2.1nmoles of polyAdenosine oligonucleotide (10-mer); red curve: H_2O + 2.1nmoles of polyThymidine oligonucleotide (10-mer); black curve: H_2O. Adapted from[12]

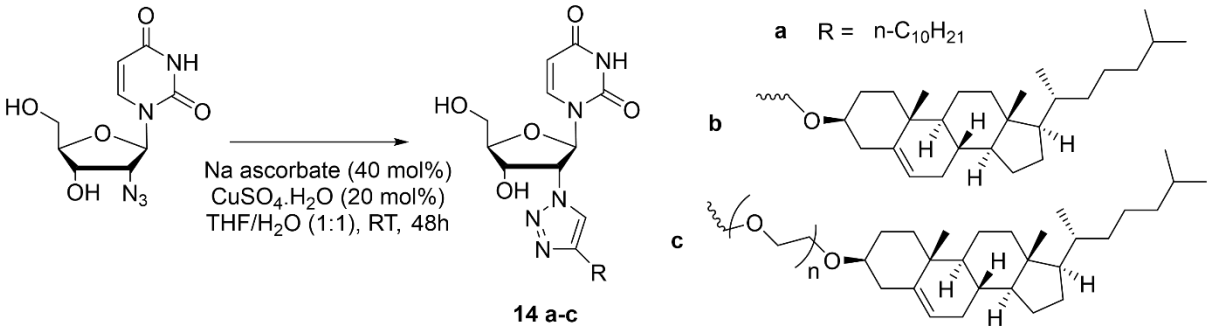

Figure 7. Synthesis approach of 2'-substituted uridine. Adapted from[13]

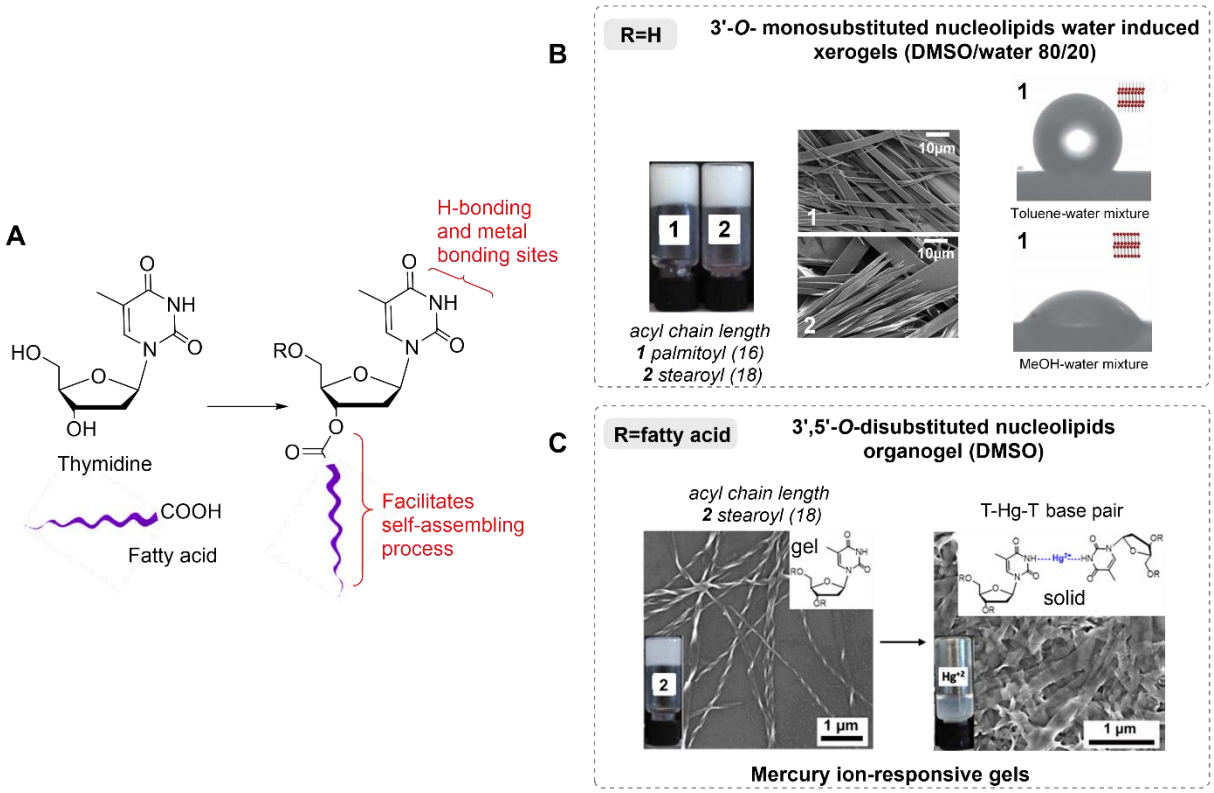

Figure 8. Supramolecular gels based on nucleolipids **A.** NLs chemical structures. **B.** 3'-*O*-monosubstituted xerogels 1 and 2 gelation tests (DMSO/water 80/20), FESEM images of 1 (up; scale bar: 10µm) and 2 (down; scale bar: 10µm) and contact angle images of water droplets on the surface of 1 fabricated from toluene-water mixture (up) and methanol-water mixture (down). **C.** 3', 5'-*O*-disubstituted 2 gelation tests and FESEM images without (left) and with mercury ions (right). Adapted from[14]

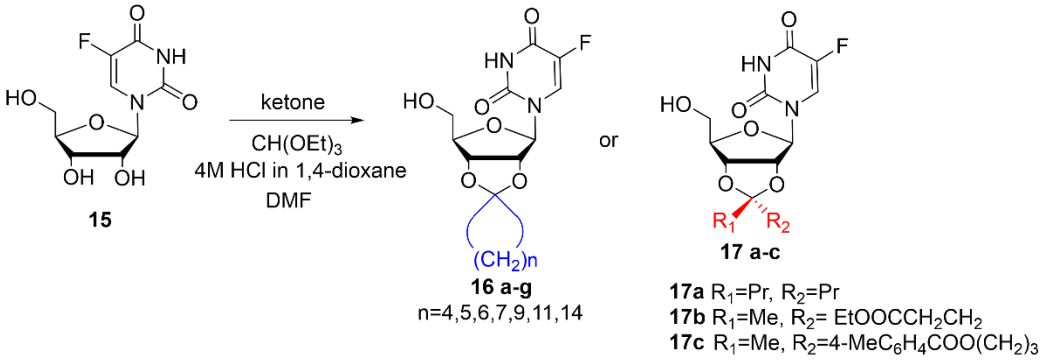

Figure 9. Synthetic pathway of *O*-2',3'-ketal 5-fluorouridine derivatives. Adapted from[15]

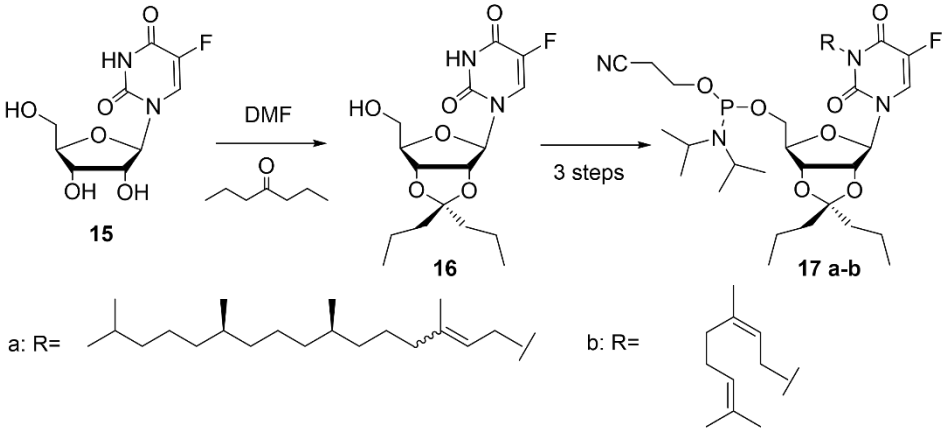

Figure 10. Synthetic pathway of nucleoterpenes. Adapted from[18]

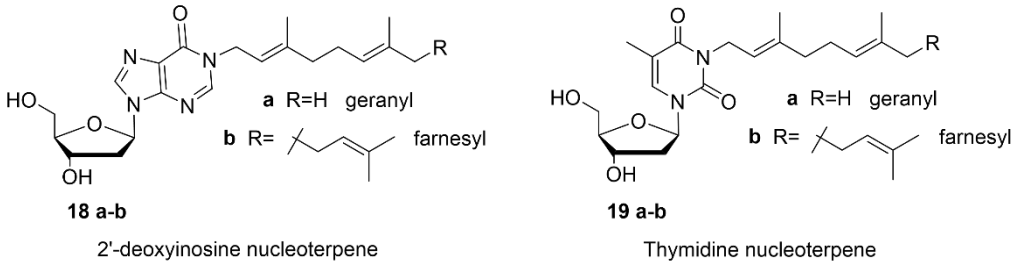

Figure 11. Molecular structures of 2'-deoxyinosine and thymidine nucleoterpenes. Adapted from[19]

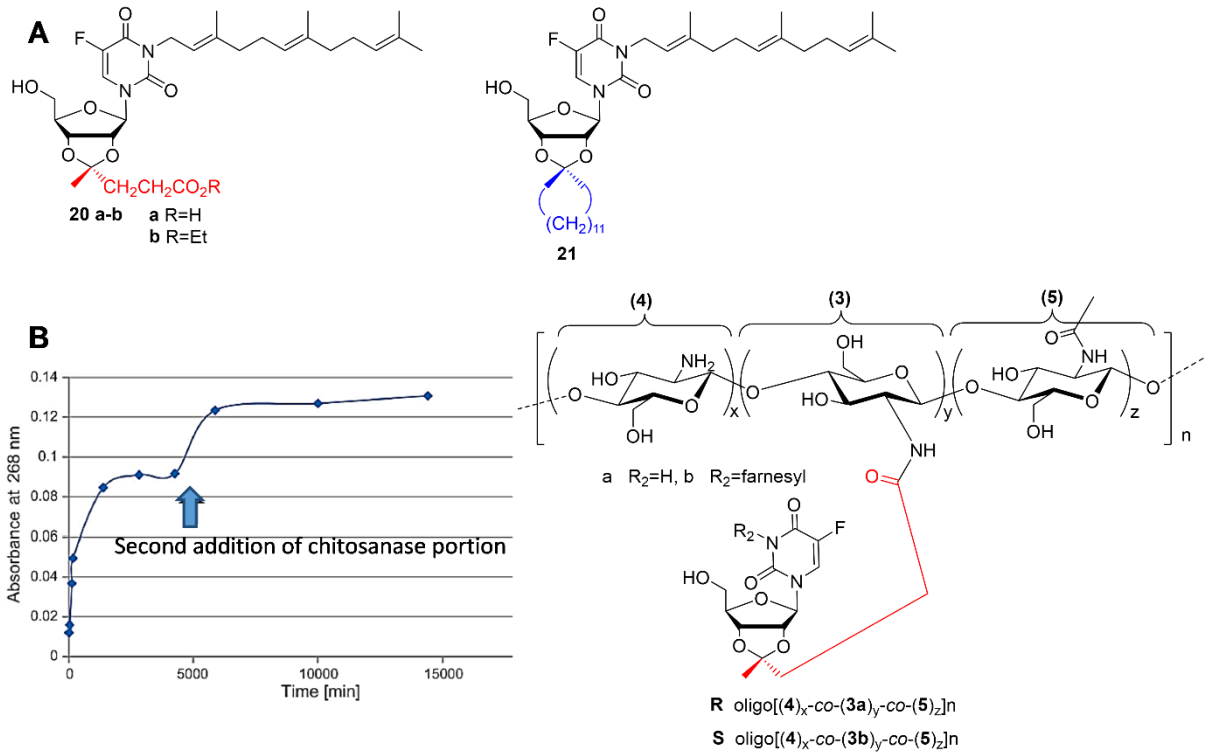

Figure 12. Covalent immobilization of farnesylated nucleolipids on chitosans **A.** NLs chemical structures. **B.** Chitosanase-catalyzed degradation of a 5-fluorouridine chitosan-foil conjugate as a function of time. Adapted from[20]

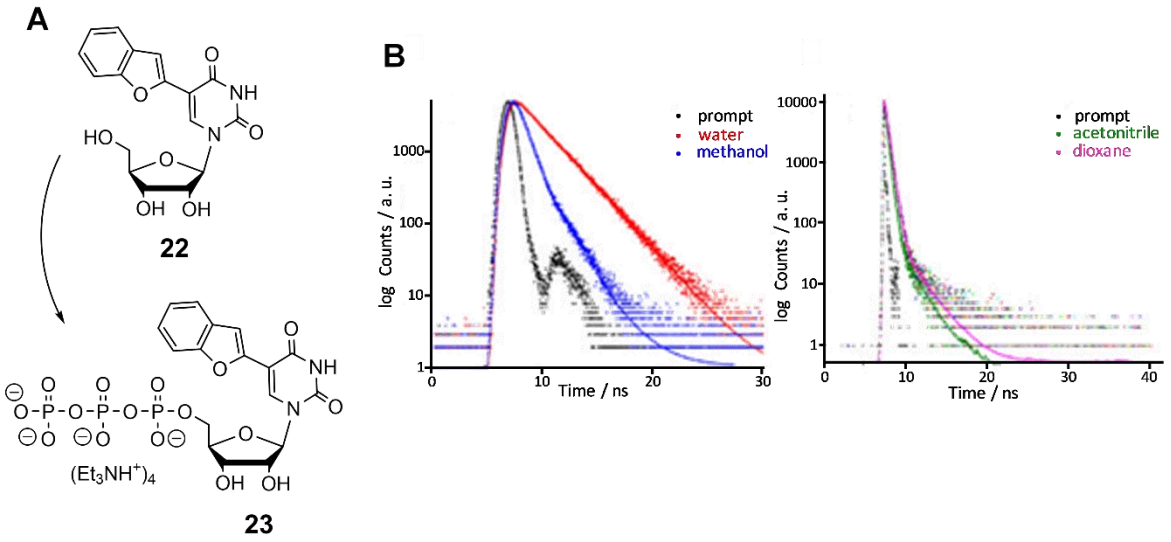

Figure 13. Fluorescent pyrimidine ribonucleoside analogue **A.** Chemical structures of probes **22** and **23**. **B.** Excited state decay profile of ribonucleoside **5** in water (red), methanol (blue), acetonitrile (green) and dioxane (pink). Laser profile in black (prompt). Adapted from[23]

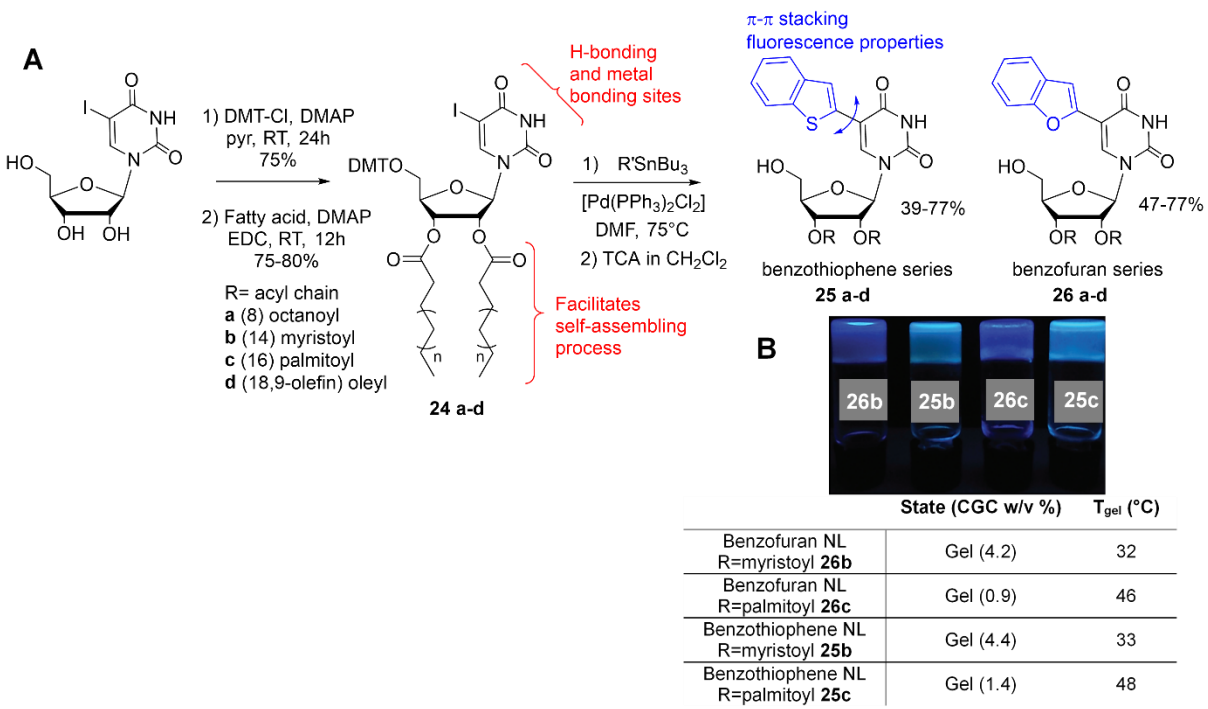

	State (CGC w/v %)	T_{gel} (°C)
Benzofuran NL R=myristoyl **26b**	Gel (4.2)	32
Benzofuran NL R=palmitoyl **26c**	Gel (0.9)	46
Benzothiophene NL R=myristoyl **25b**	Gel (4.4)	33
Benzothiophene NL R=palmitoyl **25c**	Gel (1.4)	48

Figure 14. Responsive fluorescent nucleolipid gels **A.** NLs **25** and **26** synthetic pathway. **B.** Gelation properties of fluorescent NLs (down) and images under UV light (365nm, up). Adapted from[25]

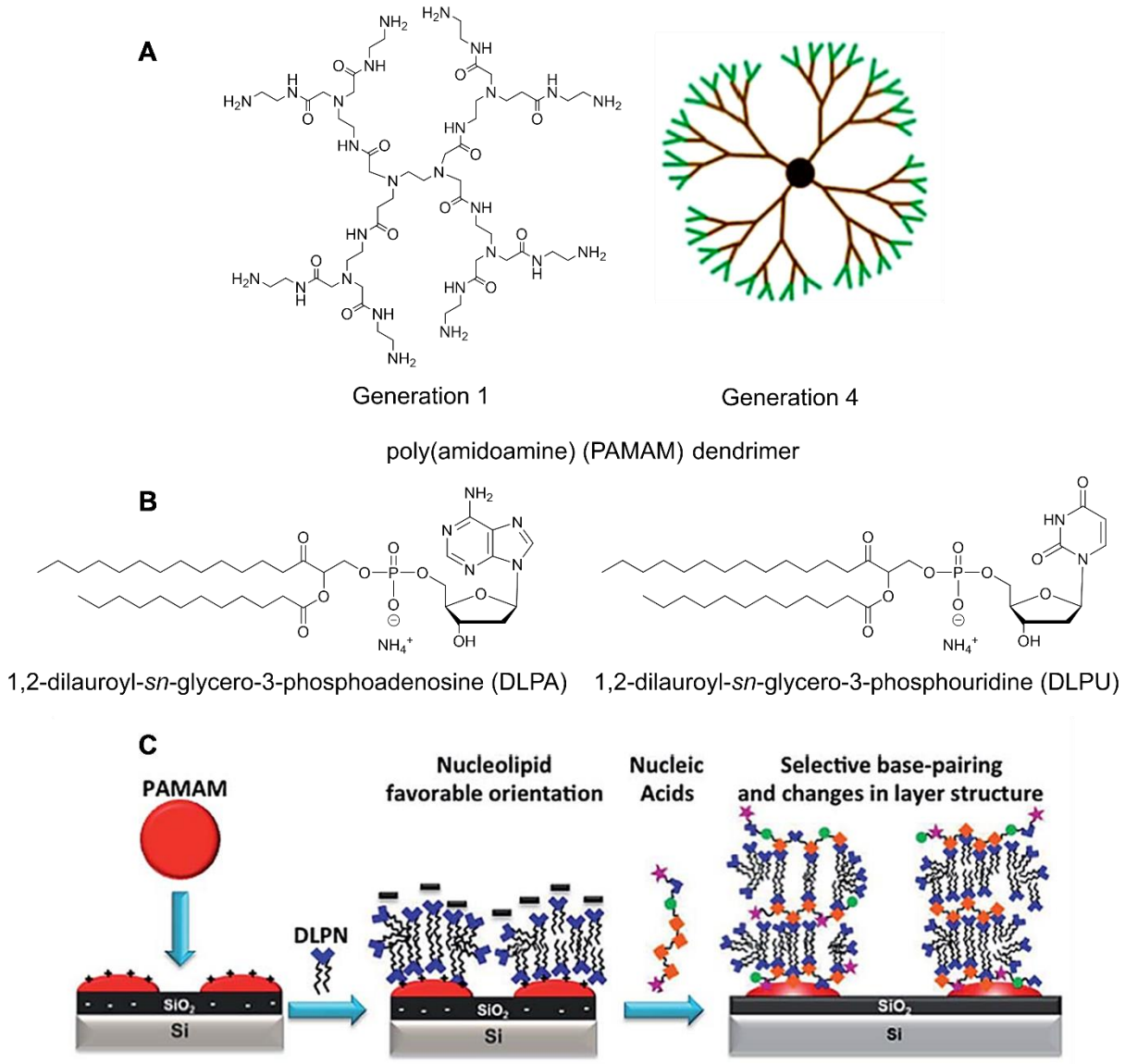

Figure 15. Dendrimer/nucleotide lipids surface films. **A.** PAMAM dendrimers. **B.** Nucleotide lipids (DLPNs), 1,2-dilauroyl-*sn*-glycero-3-phosphoadenosine (DLPA) and 1,2-dilauroyl-*sn*-glycero-3-phosphouridine (DLPU). **C.** Sequential addition of dendrimers, DLPN and nucleic acids allowing selective binding between the functionalized surface and nucleic acids. Adapted from[30,31]

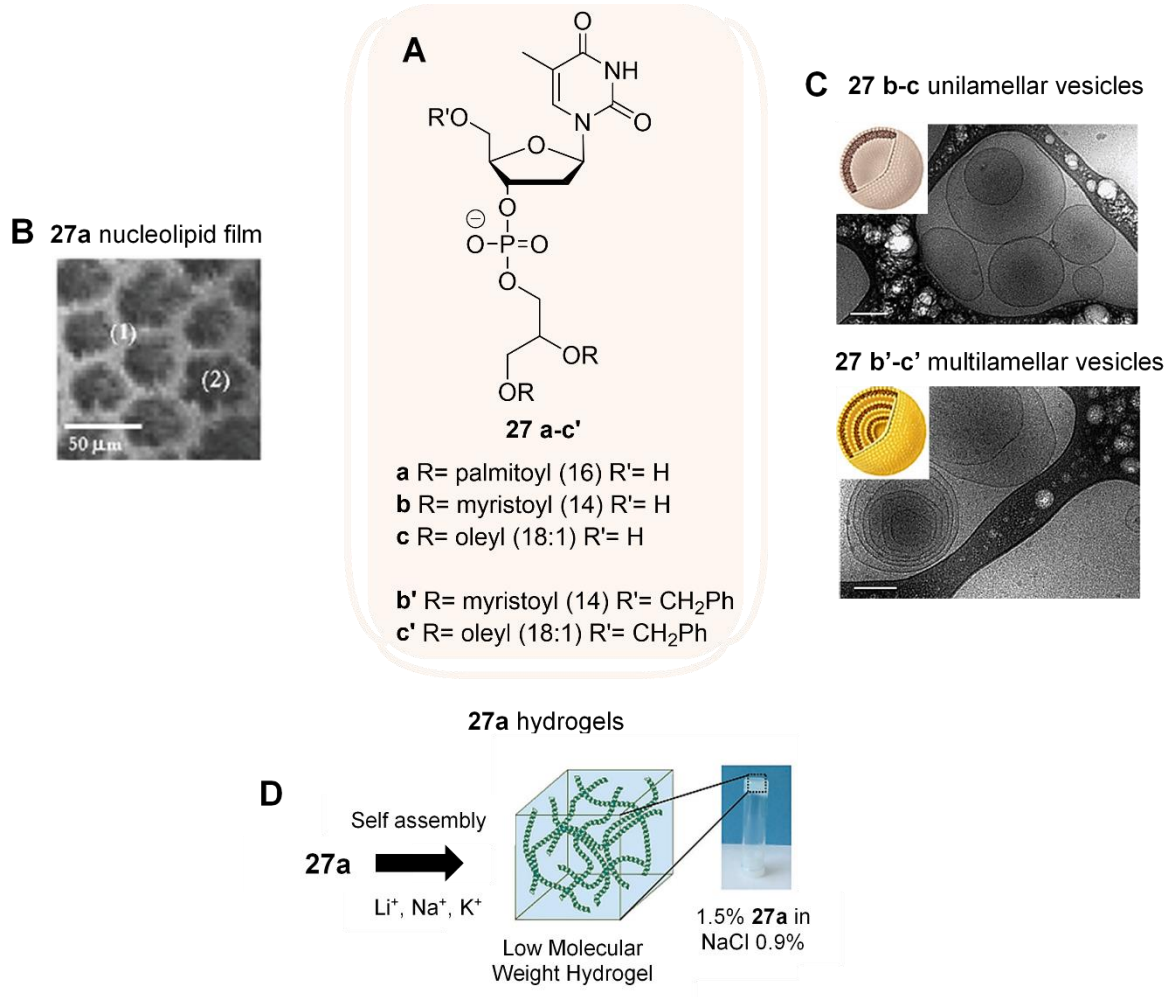

Figure 16. Colloidal properties of 1,2-diacyl-*sn*-glycerol nucleotide lipids. **A.** Chemical structures of nucleotide lipids. **B.** Ellipsometric image for a film of **27a** under compression representing (1) monolayer and (2) bilayer (scale bar: 50µm). **C.** Example of CryoTEM images of unilamellar (up) and multilamellar (down) vesicular systems formed by **27b** and **27b'** respectively (scale bar: 200nm, HEPES buffer 50mM). **D.** 1.5% low molecular weight hydrogel of **27a** formed in 0.9% NaCl in water. Adapted from[39–41]

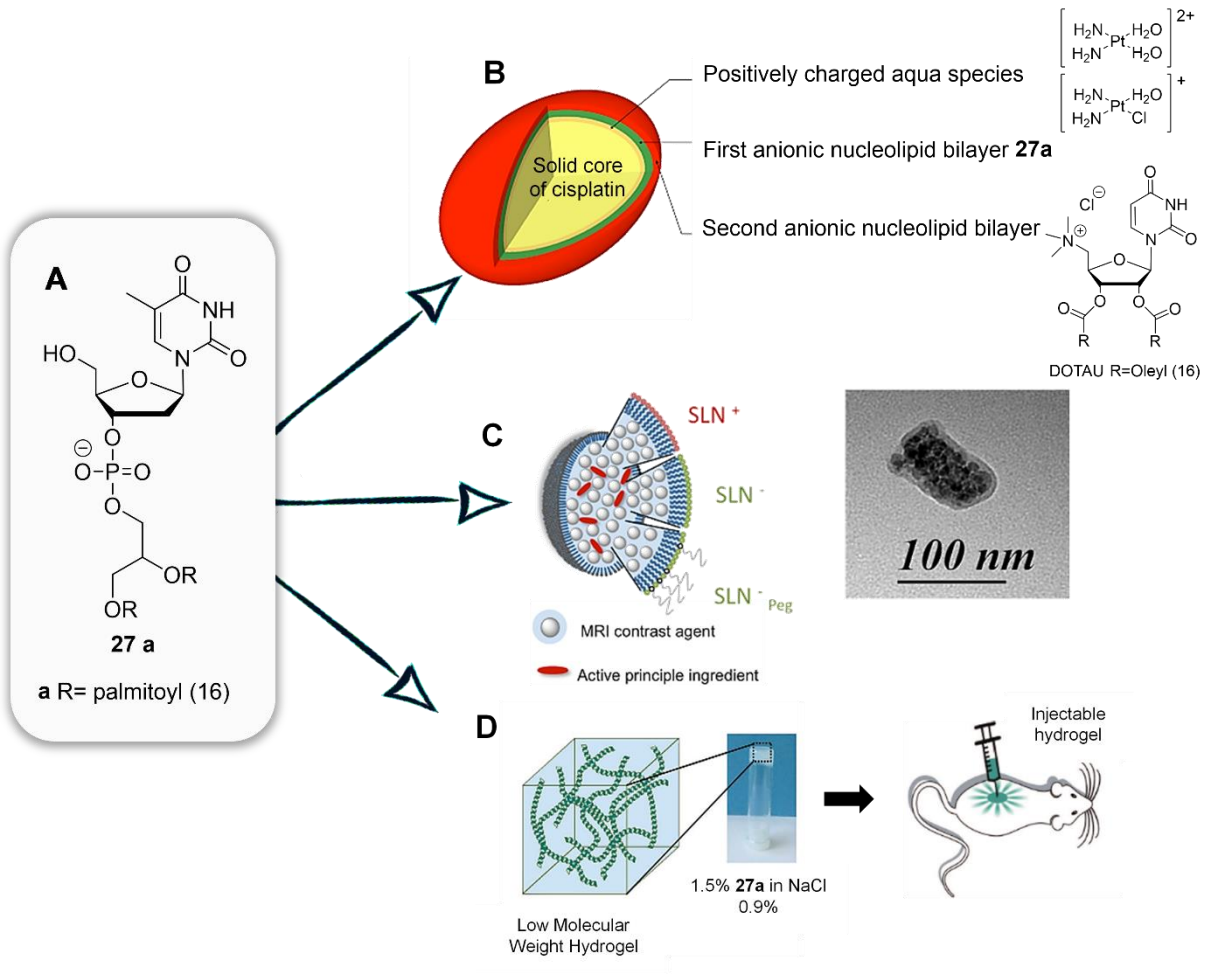

Figure 17. Examples of nucleotide lipids biomedical applications **A.** Chemical structure of **27a**. **B.** Nanoparticle schematic representation including anionic (**27a**) and cationic (DOTAU, 2',3'-dioleyl-5'-deoxy-5'-trimethylammoniumuridine) NLs. **C.** Nucleotide lipid based SLNs schematic representation (left) and TEM image of iron nanoparticles incorporated in this system (right, scale bar: 100nm). **D.** Injectable hydrogel allowing drug release. Adapted from[41,44,45]

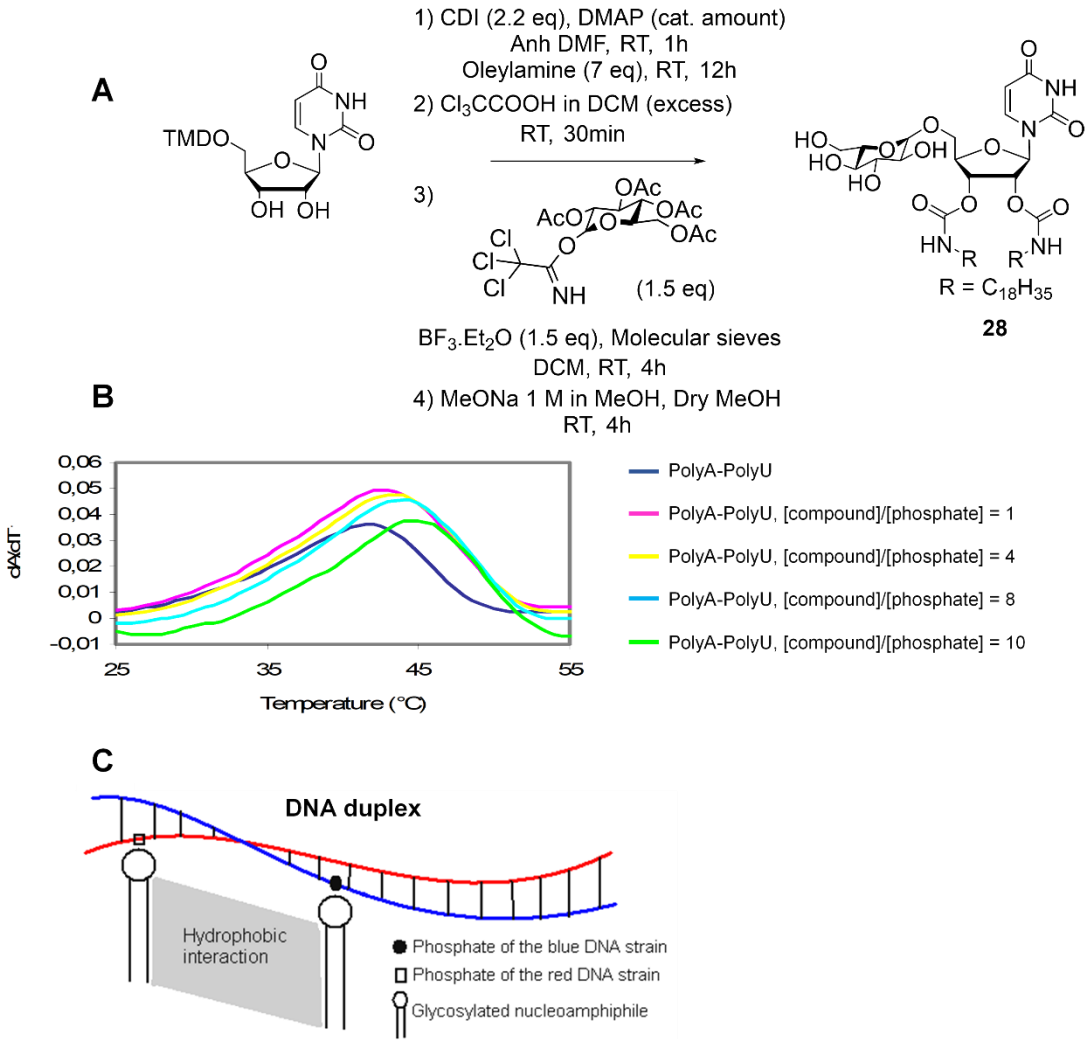

Figure 18. First designed GNL as an interesting tool for DNA stabilization. **A**. glycosyl dicarbamate Uridine synthesis. **B.** Absorbance derivative at 260nm depending on temperature of polyA-polyU in presence of increasing amounts of GNL. **C**. DNA duplex stabilization by hydrophobic interactions between lipid chains and hydrogen bonding between sugars and phosphates. Adapted from[46]

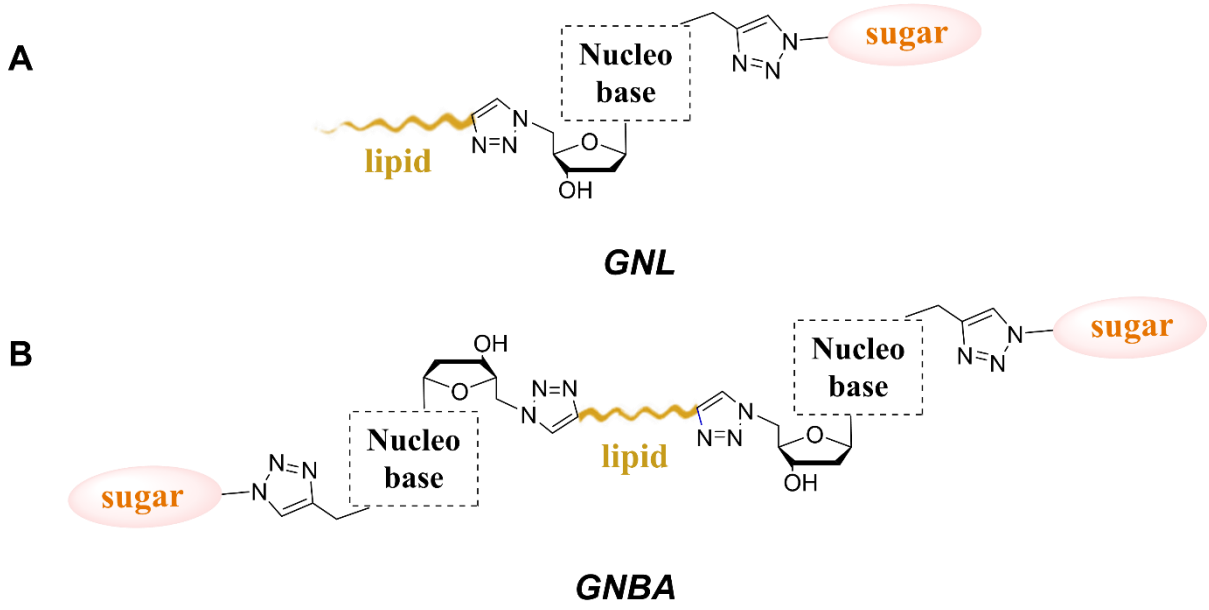

Figure 19. Schematic representation of **A**.GNL and **B**. GNBA.

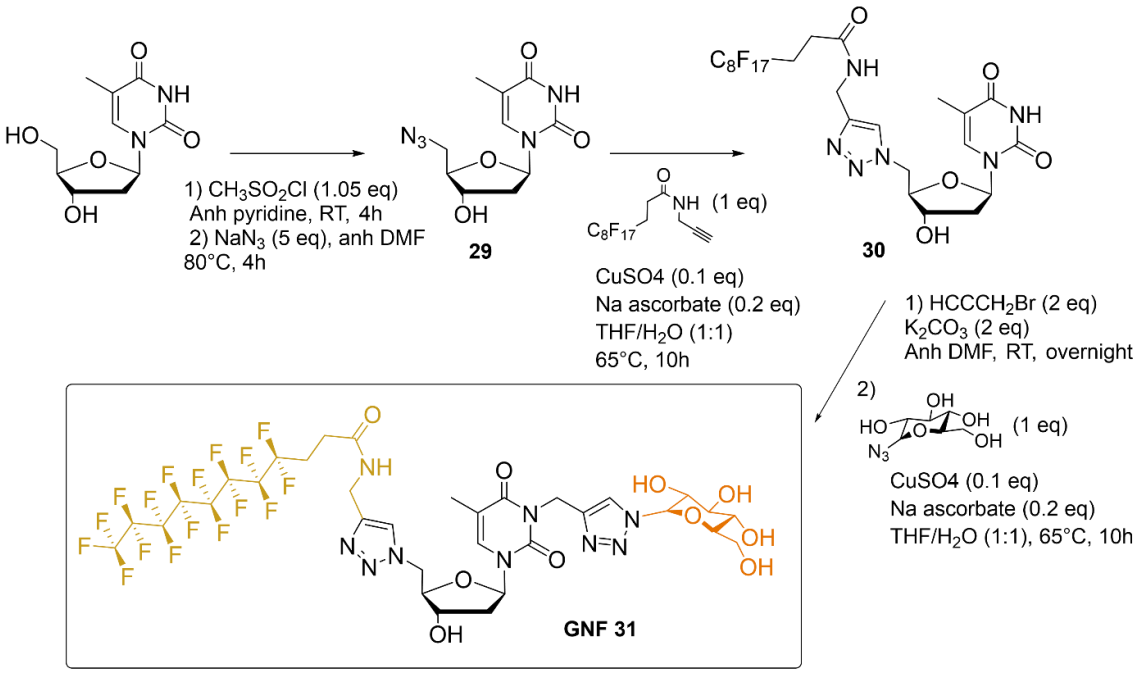

Figure 20. Synthetic route of GNF. Adapted from[52]

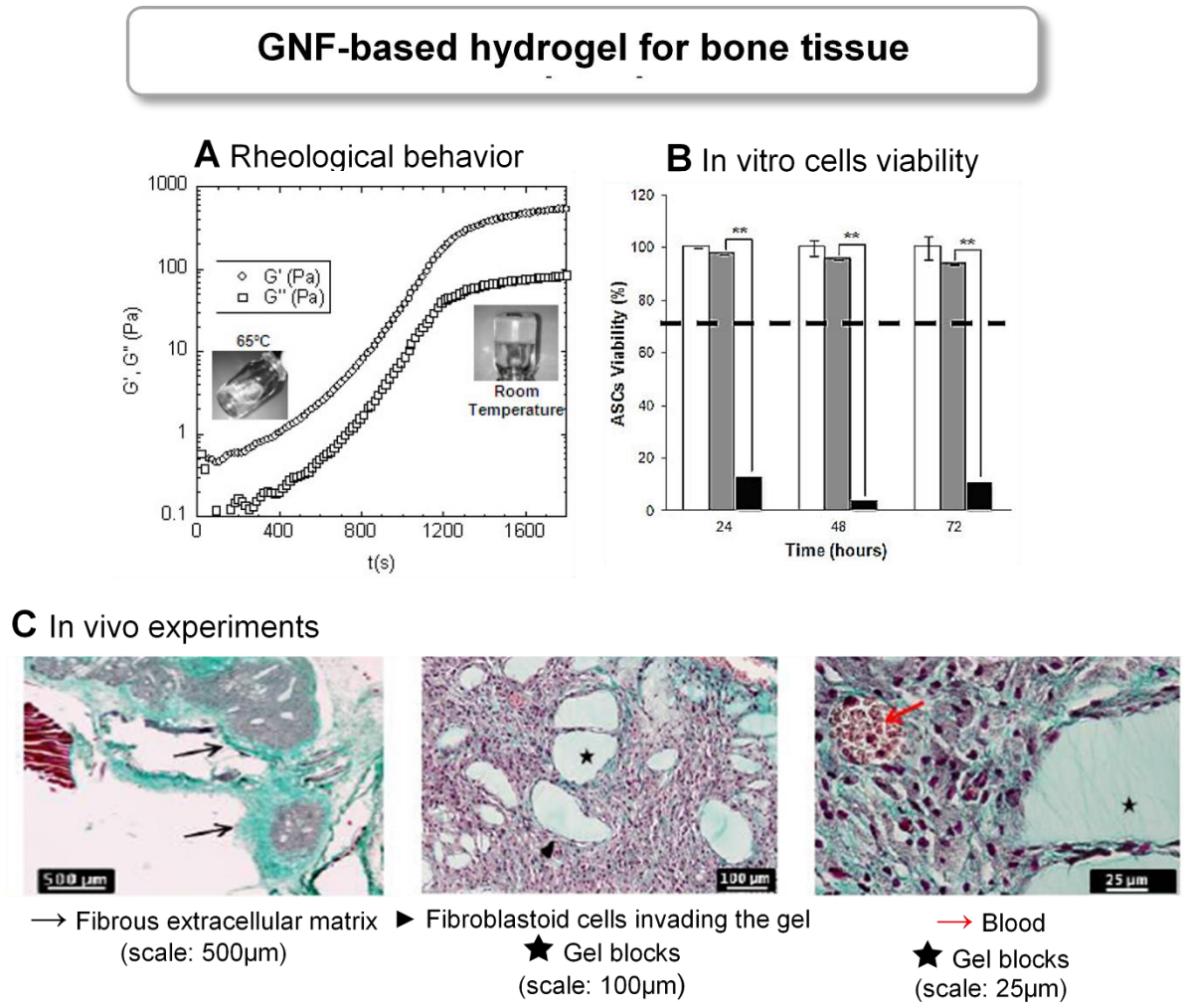

Figure 21. GNF – a promising tool for bone tissue engineering. **A**. Gelation monitoring of a 1.5 % w/v GNF-based hydrogel in PBS at RT. **B**. GNF-based hydrogel - ASCs cells viability (neutral red uptake; white bars: results; grey bars: control samples incubated with normal culture medium; black bars: phenol-treated samples; statistical analyses with Mann-Whitney U-test. **: $p < 0.01$). **C**. Histological sections of biopsies 60 days after subcutaneous implantation of GNF-based hydrogel in mice (Masson's trichrome stain). Adapted from[58]

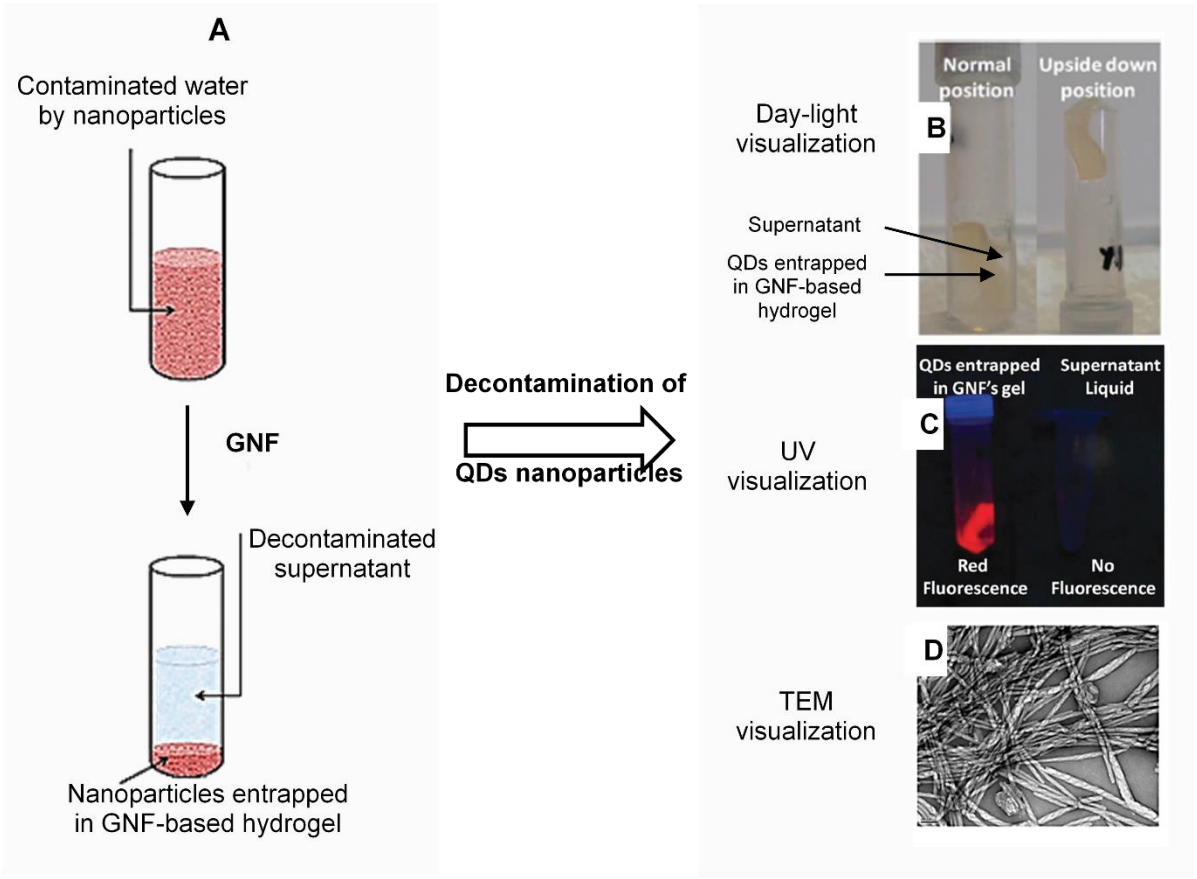

Figure 22. Nanoparticles decontamination by GNF-based hydrogel. **A**. Schematic illustration of the decontamination process. **B**. QDs entrapped in GNF-based hydrogel 0.1% w/v in contaminated water in normal and upside down positions. **C**. UV visualization of the supernatant and QDs entrapped in the gel (λmax= 312nm). **D**. TEM image showing entrapped QDs in the hydrogel (scale bar: 100nm). Adapted from[59]

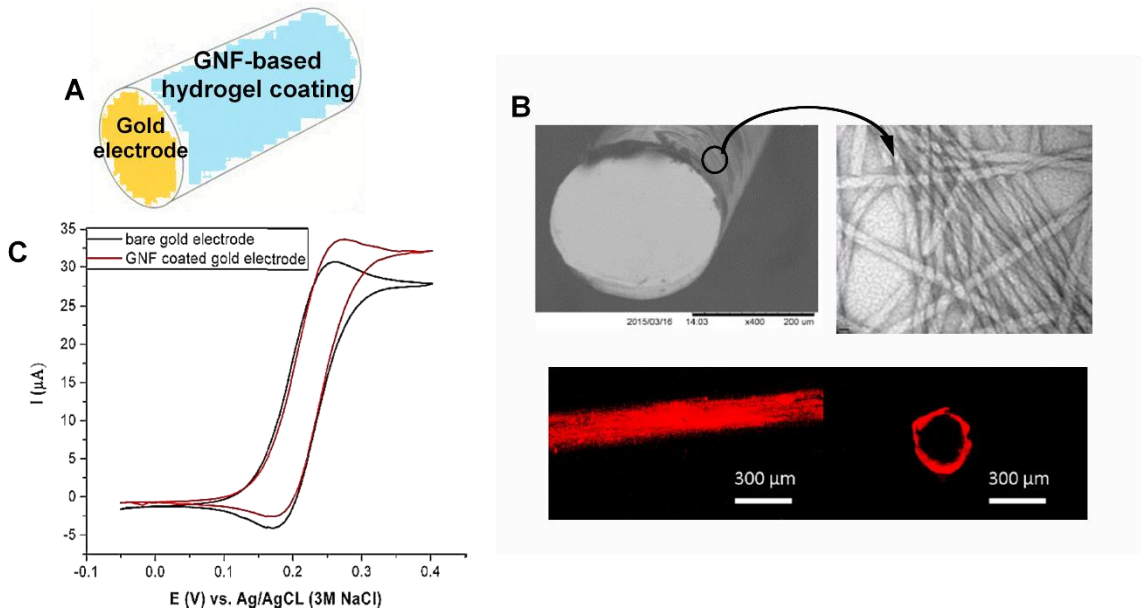

Figure 23. Hybrid GNF-based hydrogel macroporous electrode. **A**. Schematic representation of the hybrid electrode. **B**. SEM image of the crossing section of the coated electrode (left), TEM image of GNF-based hydrogel (scale bar: 100nm, right) and fluorescence microscope image of GNF-based hydrogel / rhodamine

coating on the electrode (λ= 512nm, scale bar: 300µm, down). **C**. Cyclic voltammetry of electrodes without (black line) and with hydrogel (red line). Adapted from[60]

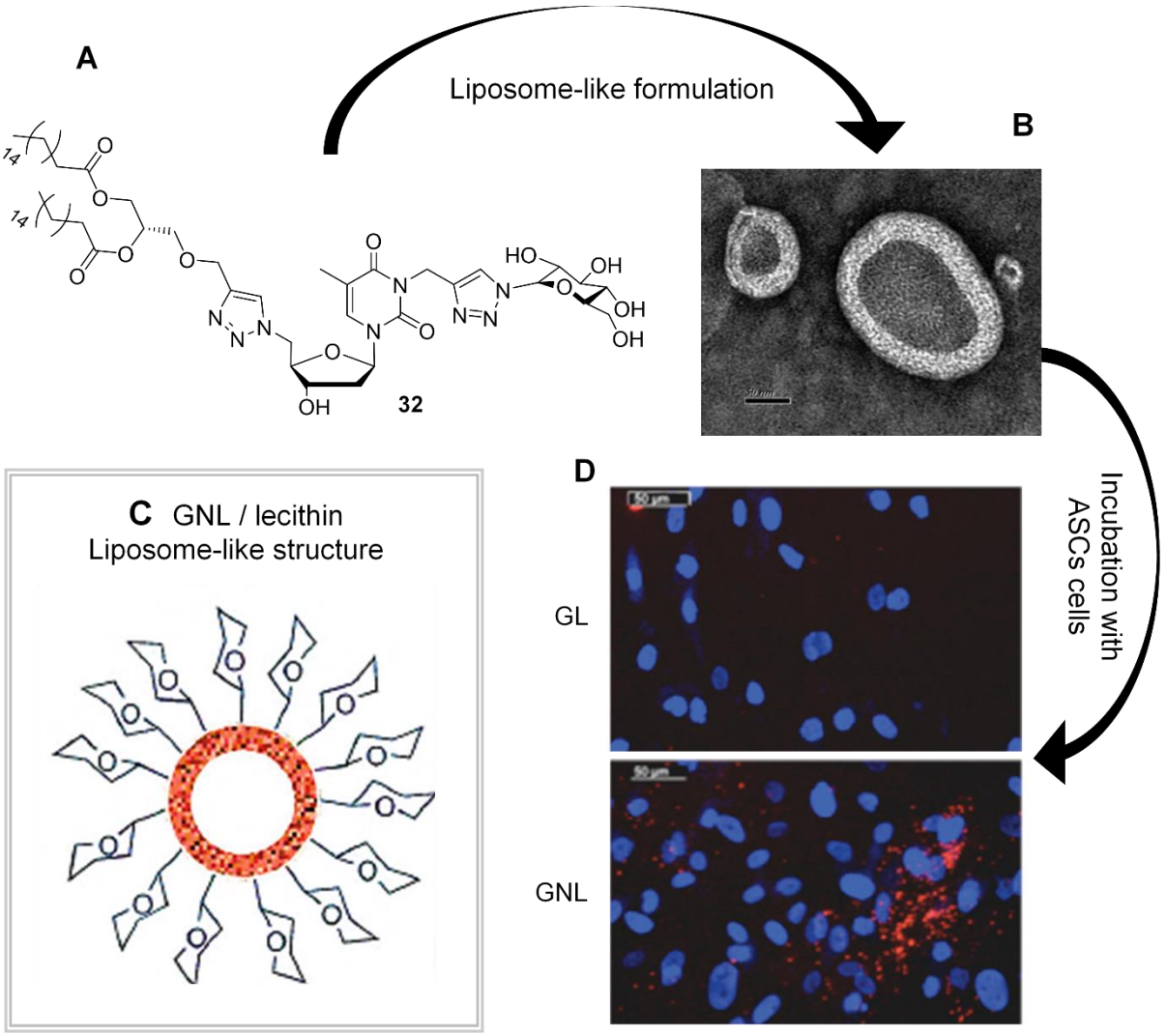

Figure 24. GNL liposome-like structure as drug delivery system. **A**. GNL structure. **B**. TEM image of liposome-like structure (scale bar: 50nm). **C**. Schematic representation of liposome-like structure. **D**. Confocal microscopy showing the internalization of DIL-labeled GL-containing liposome (top) and GNL-containing liposome (bottom) in ASCs; nuclei stained in blue (scale bar: 50µm). Adapted from[53]

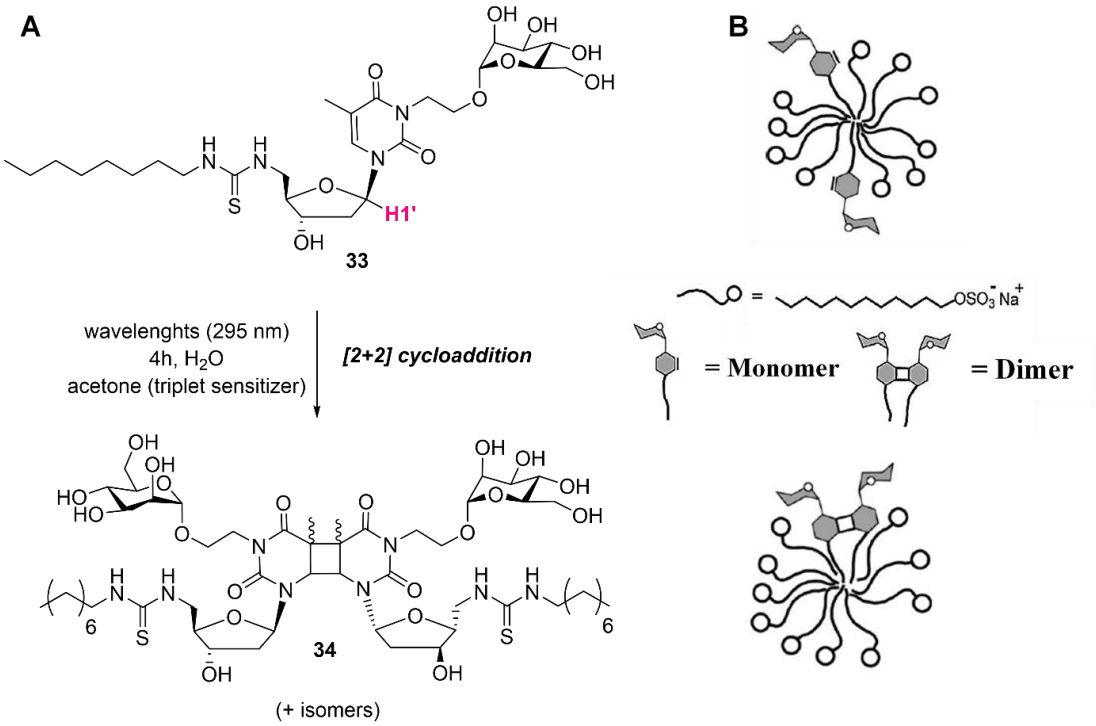

Figure 25. Photoswitchable glycothymidines. **A.** Molecular structures of monomers (up) and dimers (down). **B.** Schematic representation of incorporated monomers into SDS micelles and then photodimerised inside the structure. Adapted from[61]

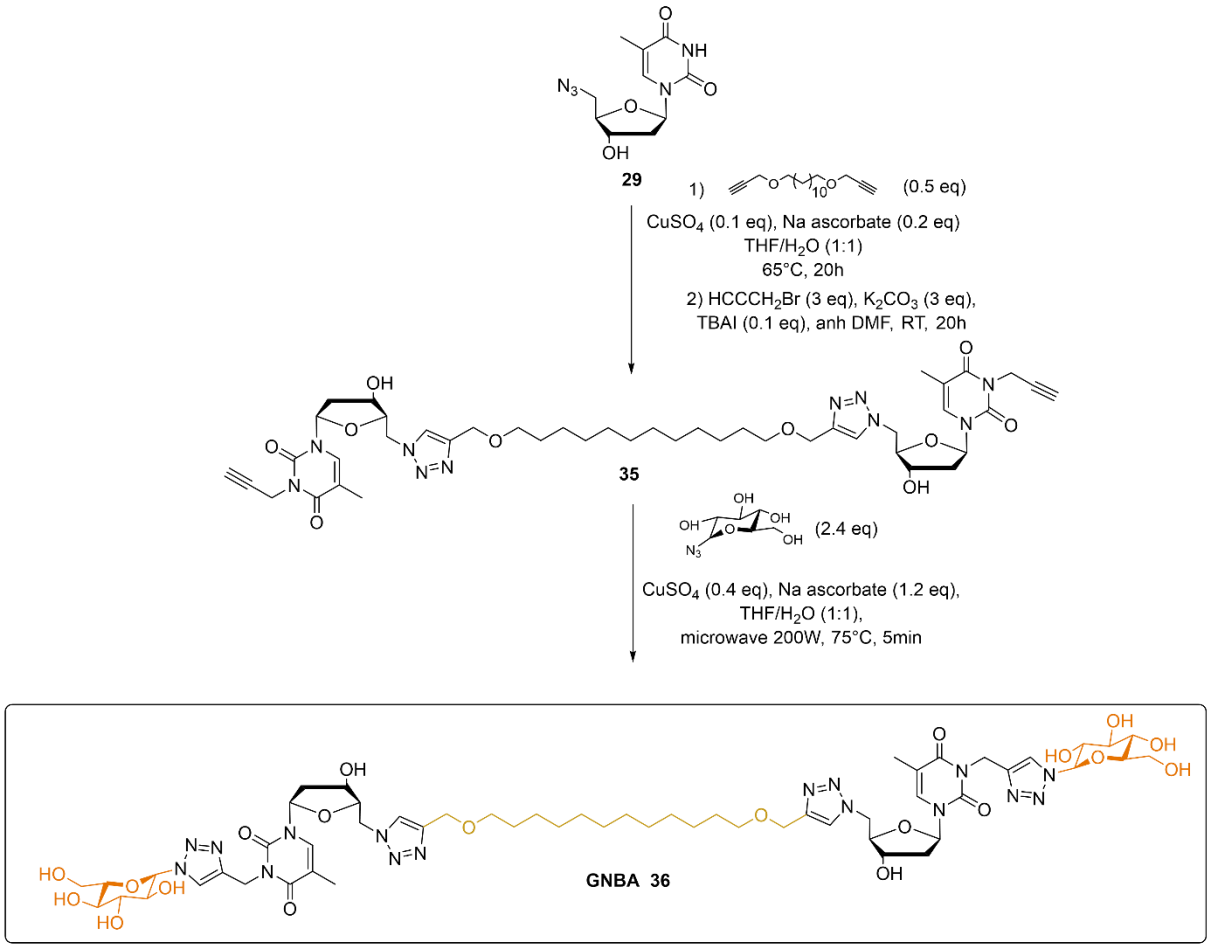

Figure 26. Synthesis of GNBA. Adapted from[55]

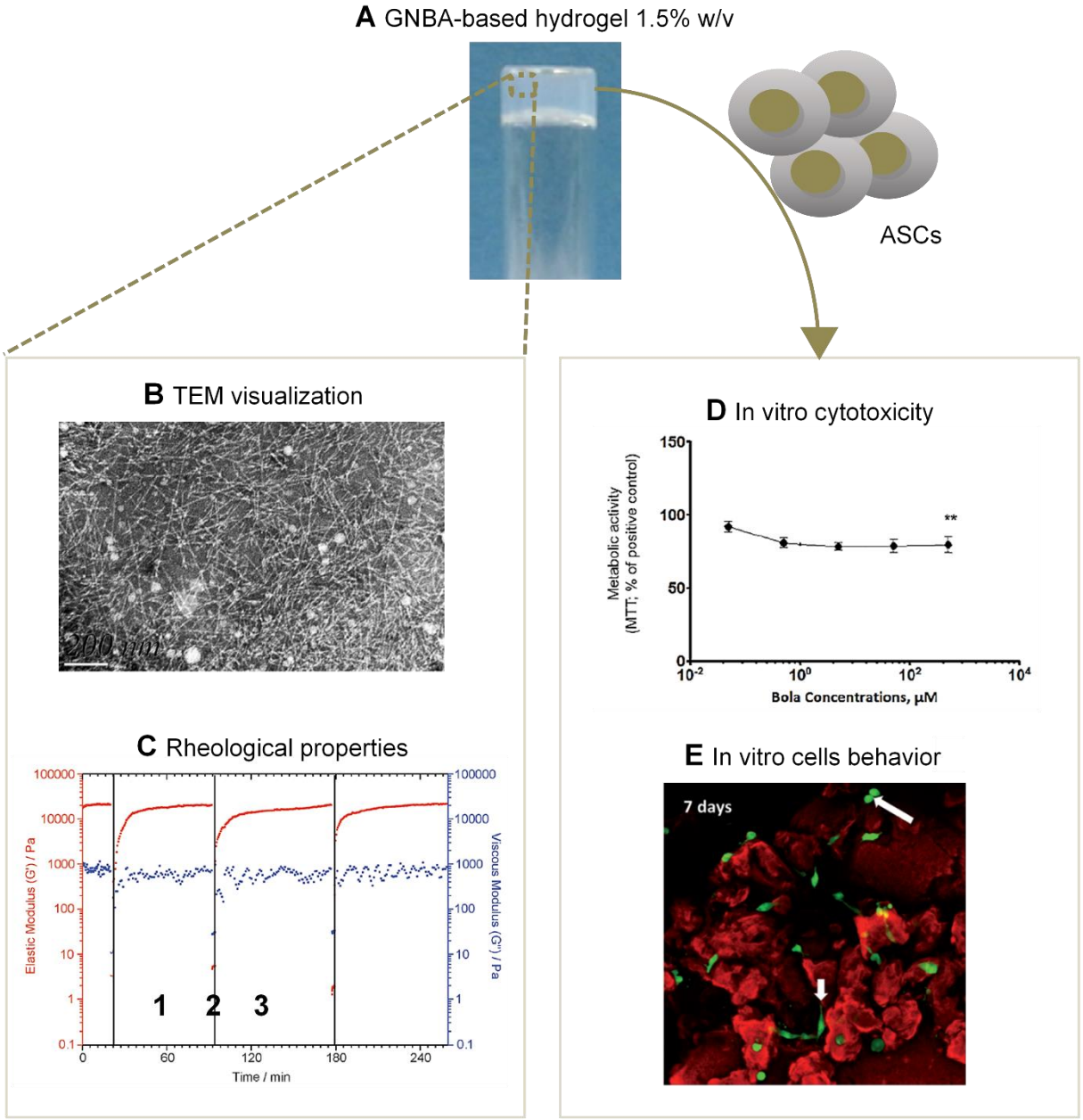

Figure 27. GNBA-based hydrogel as an extracellular matrix substitute. **A**. GNBA-based hydrogel 1.5% w/v. **B**. Hydrogel TEM image with fibers around 6-9nm in width (scale bar: 200nm). **C**. Thixotropic properties of the hydrogel (1% w/v concentration) at a fixed angular frequency of 6.283rad.s^{-1} (1. 0.03% strain for 20min; 2. 15% strain for 2min; 3. 0.03% strain until the return of the initial gel state). **D**. In vitro cells metabolic activity evaluated by MTT assays in human ASCs after 72 hours of incubation with increasing concentration of GNBA-based hydrogel. **E**. Confocal macroscopy image of GNBA-based hydrogel (3% w/v concentration) embedded human ASCs after 7 days; top white arrow: dividing cell; bottom white arrow: fibroblastoid cell. Cells stained in green (calcein) and GNBA-based hydrogel in red (ethidium) (scale bar: 200µm). Adapted from[55]

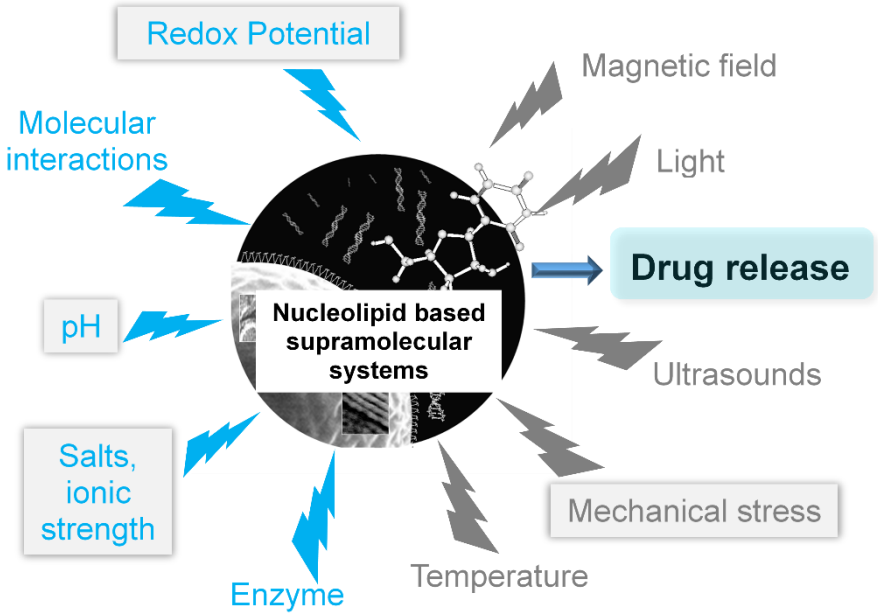

Figure 28. Schematic drawing illustrating the release of a drug from nucleolipid based supramolecular systems upon different stimuli, either external (in gray) or internal (in blue). Grays frames indicate stimuli investigated with NLs and GNLs.

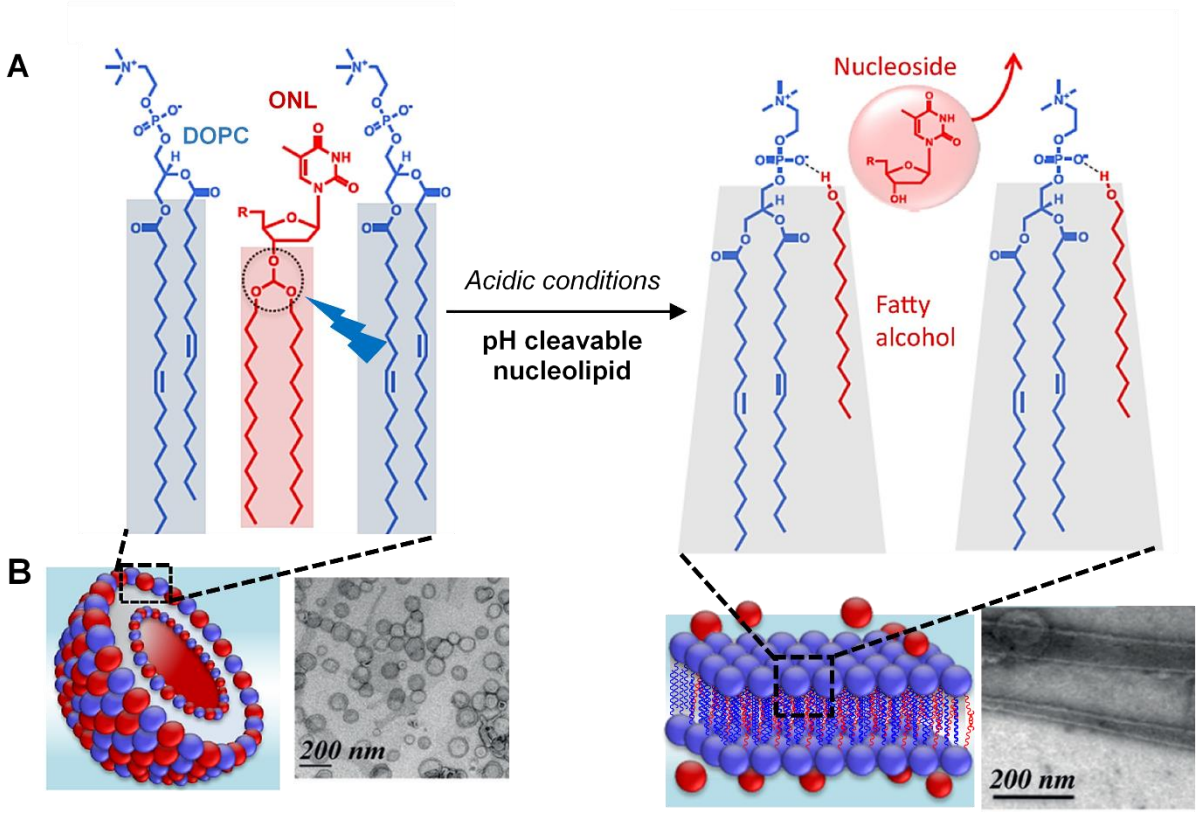

Figure 29. pH cleavable nucleolipid. **A.** Chemical structures of ONL/DOPC before (left) and after (right) cleavage of orthoester function (dotted line) in acidic conditions. **B.** Schematic representation and TEM image of

ONL/DOPC liposomes (left, scale bar: 200nm) and their destabilization (right, scale: 200nm) in acidic conditions (case of anionic ONL). Adapted from[82]

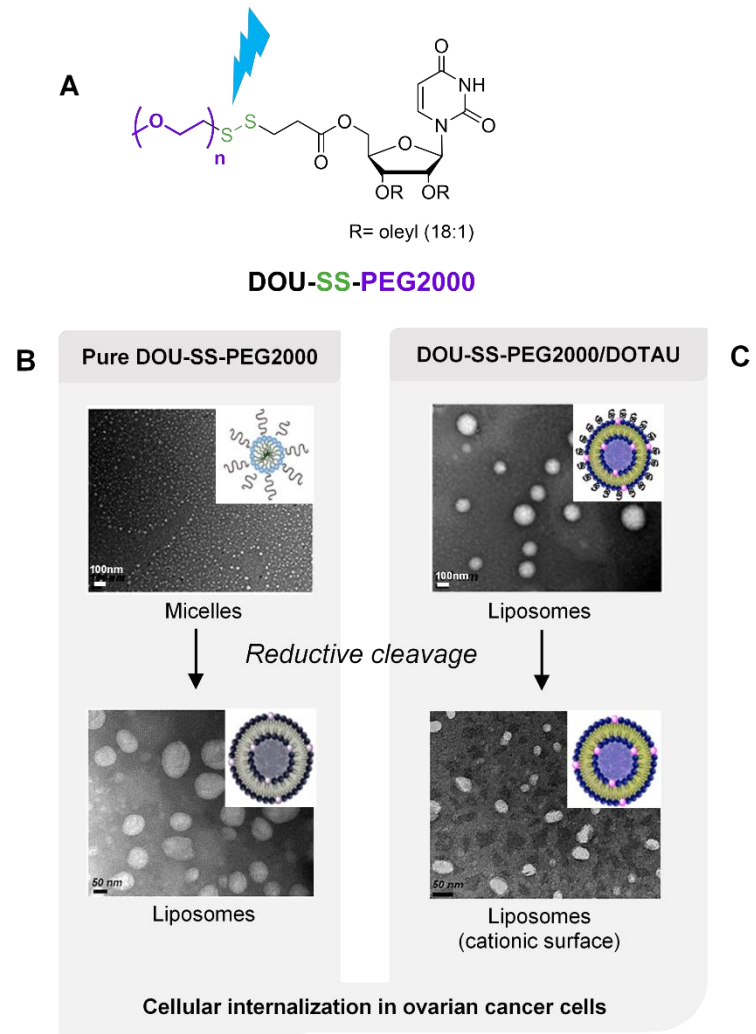

Figure 30. Cleavable PEG-based nucleolipid. **A.** Chemical structure of DOU-SS-PEG2000. **B.** TEM images of NL self-assembly to form micelles (up, scale bar: 100nm) and liposome (down, scale bar: 50nm) after a reductive cleavage of PEG moieties. **C.** TEM images of NL/DOTAU self-assembly to liposomes (up, scale bar: 100nm) and naked liposome (down, scale bar: 50nm) after the reductive. Adapted from[85]

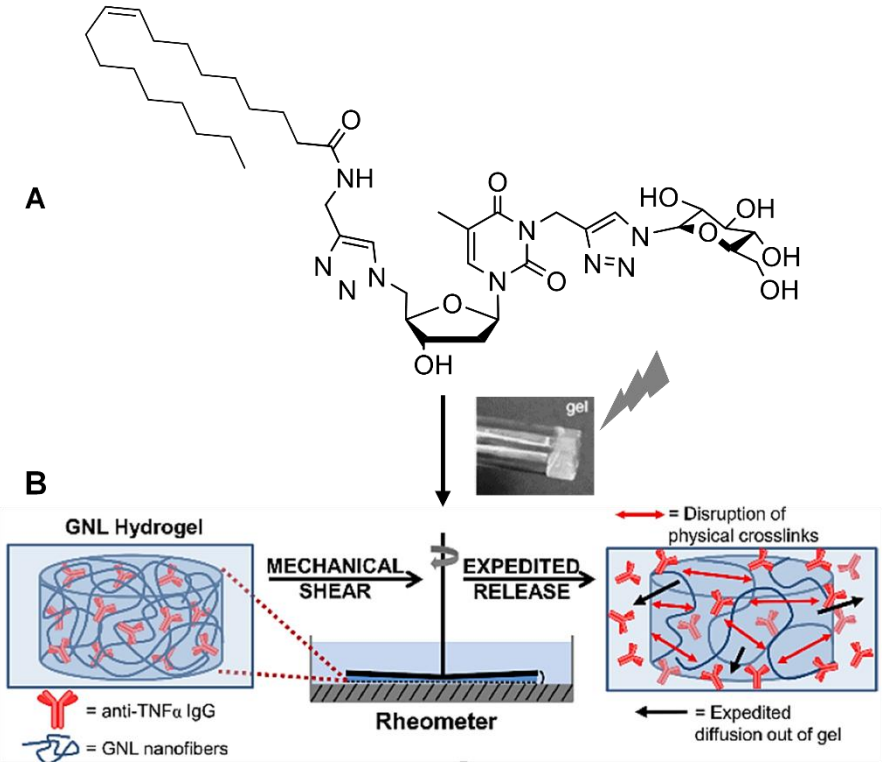

Figure 31. Mechanoresponsive hydrogel. **A.** GNL chemical structure[50]. **B.** Schematic representation of the control release of anti-TNFα entrapped in the hydrogel upon mechanical stress. Adapted from[92]

Biographies

Dr. Valérie Desvergnes received her Ph.D in chemistry from the University of Lyon 1, France in 1999. After a postdoctoral fellowship in the group of Professor Jérome Lacour (University of Geneva), she was appointed CNRS researcher at the Institute of Organic and Analytic Chemistry (ICOA, Orléans, France) in 2002. Her research topic was the design, synthesis and biological evaluation of innovative iminosugar nucleotides as antimycobacterial compounds. After several years at the Institute of Molecular Sciences (ISM, Bordeaux, Professor Yannick

Landais' group), she joined Professor Philippe Barthélémy's team in 2016, where she develops new biomimetic organocatalyzed synthetic pathways to nucleoconjugates (nucleolipids, glyconucleolipids…).

Dr. Laurent Latxague received his Ph.D in chemistry focused on glucosinolates from the University Bordeaux I, France, in 1991, and continued his work in the group of Professor Dr. Joachim Thiem (Hamburg, Germany). He was appointed Associate Professor at the University Bordeaux 2 in 1993 in the group of Professor Gérard Déléris and was involved in the synthesis of organosilicon analogs of acyclic nucleosides. He then moved to Professor Laurence Bordenave's group (INSERM U577) in 2005 to work on biodelivery systems relating to bone regeneration. In 2011 he joined Professor Philippe Barthélémy's group to develop supramolecular hydrogels for tissue engineering.

Prof. Philippe Barthélémy received his PhD in chemistry from the University of Montpellier II, France in 1993. Then he was a postdoctoral fellow at Emory University in the group of

Prof. Fredric Menger (Lavoisier Grant). He was appointed as Associate Professor at the University of Avignon in 1996. Barthélémy was visiting Associate Professor at Duke University in 2001. In 2005 he was appointed as full Professor at the University of Bordeaux Segalen, where he became Vice President of the University in 2011. He is leading "ChemBioPharm" team of INSERM U1212. Over the course of his tenure, Barthélémy's research on bioinspired systems has yielded more than 130 peer-reviewed publications, 20 patents, and 110 invited conferences/presentations.

Table of contents:

Hybrid molecules combining nucleic acid structures with lipids have recently received increasing attention as a new class of supramolecular biomaterials. An overview of the latest studies on their chemical and biological properties is presented, including several biomedical applications ranging from medicinal chemistry to biomaterials. Some suggestions for developing this type of soft materials in the near future are also proposed.

Keywords: Nucleosides, Lipids, Amphiphiles, supramolecular assemblies, Hydrogels

Julie Baillet, Valérie Desvergnes, Aladin Hamoud, Laurent Latxague, and Philippe Barthélémy

Lipid and nucleic acid chemistries: combining the best of both worlds to construct advanced materials

ToC figure: